“Scalable Light Module for Low-Cost, High-Efficiency Light-Emitting Diode Luminaires”

Dept. of Energy
National Energy Technology Laboratory

Final Technical Report

Period Start Date:	**August 1, 2013**
Period End Date:	**August 31, 2015**
Principal Investigator:	**Eric Tarsa** **(805) 690-3603, eric_tarsa@cree.com**
Date Report Issued:	**November 30, 2015**
Award Number:	**DE-EE0006264**
Project Manager:	**Joel Chaddock**

CREE, Inc.
Santa Barbara Technology Center
340 Storke Road
Goleta CA 93117
(805) 968-9460
DUNS 183252501

EXECUTIVE SUMMARY

During this two-year program Cree developed a scalable, modular optical architecture for low-cost, high-efficacy light emitting diode (LED) luminaires. Stated simply, the goal of this architecture was to efficiently and cost-effectively convey light from LEDs (point sources) to broad luminaire surfaces (area sources). By simultaneously developing warm-white LED components and low-cost, scalable optical elements, a high system optical efficiency resulted. To meet program goals, Cree evaluated novel approaches to improve LED component efficacy at high color quality while not sacrificing LED optical efficiency relative to conventional packages. Meanwhile, efficiently coupling light from LEDs into modular optical elements, followed by optimally distributing and extracting this light, were challenges that were addressed via novel optical design coupled with frequent experimental evaluations. Minimizing luminaire bill of materials and assembly costs were two guiding principles for all design work, in the effort to achieve luminaires with significantly lower normalized cost ($/klm) than existing LED fixtures.

Chief project accomplishments included the achievement of >150 lm/W warm-white LEDs having primary optics compatible with low-cost modular optical elements. In addition, a prototype Light Module optical efficiency of over 90% was measured, demonstrating the potential of this scalable architecture for ultra-high-efficacy LED luminaires. Since the project ended, Cree has continued to evaluate optical element fabrication and assembly methods in an effort to rapidly transfer this scalable, cost-effective technology to Cree production development groups. The Light Module concept is likely to make a strong contribution to the development of new cost-effective, high-efficacy luminaries, thereby accelerating widespread adoption of energy-saving SSL in the U.S.

DISCLAIMER

TABLE OF CONTENTS

PROJECT OBJECTIVES

Cree conducted an ambitious two-year program to develop a low-cost, low-profile, modular optical architecture that would facilitate entirely new classes of ceiling and wall lighting, as well as provide efficient alternatives for conventional form factors such as troffer retrofits. The luminaire architecture was envisioned to comprise of a flexible arrangement of Light Modules, each having high optical efficiency (exceeding 90%) and exceptional luminance uniformity in a low-cost, compact profile. A key enabling element of this lighting architecture was the development of LED components having a combination of excellent color rendering and high efficacy in a very small footprint. This effort established a high-efficacy product platform that will accelerate solid state lighting (SSL) adoption by enabling new, value–added, ultra-low profile luminaire designs and providing a superior alternative for conventional replacement applications. In Fig. 1 the key features of the program are depicted, as grouped by focus area. Each of these features and the technical approaches to achieve them are discussed in more detail below.

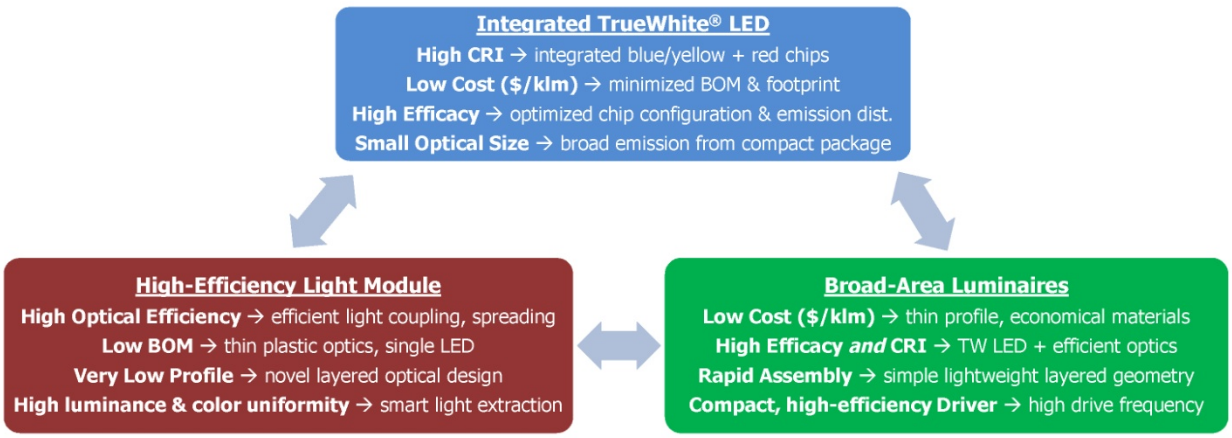

Fig. 1. Key features and technology approaches of this SSL manufacturing development program, grouped by the three primary focus areas. These areas were interdependent and vertically integrated, enabling the development of a new class of broad-area luminaires.

PROJECT ACTIVITIES

Task 2: Compact High-CRI LED Development

High refractive index composites

The luminous efficacy of LEDs is directly impacted by the efficiency of light extraction from the chip itself, and from the package lens to its surroundings. LED materials Cree uses such as (Al,In)GaN and SiC have refractive index (RI) values (~2.40 and 2.65, respectively), giving them a low critical angle at an interface with air. The use of encapsulants such as silicone (RI typically ~1.40-1.55) raises the chip light extraction efficiency by increasing the amount of light that escapes from the chip instead of encountering multiple bounces and likely re-absorption). This, combined with surface texturing or chip shaping (*e.g.* Cree's DA chip family) has enabled Cree to achieve blue light extraction efficiency (LEE) of ~80%.

To reach even higher light extraction efficiency values we desire an LED encapsulant with higher RI, but this is limited in conventional polymer encapsulant materials. We therefore investigated alternate materials, as well as modifications to existing high-performance silicones. The latter was accomplished via addition of a high-RI solid phase to the silicone matrix, such that the composite had an enhanced RI without scattering or absorption.

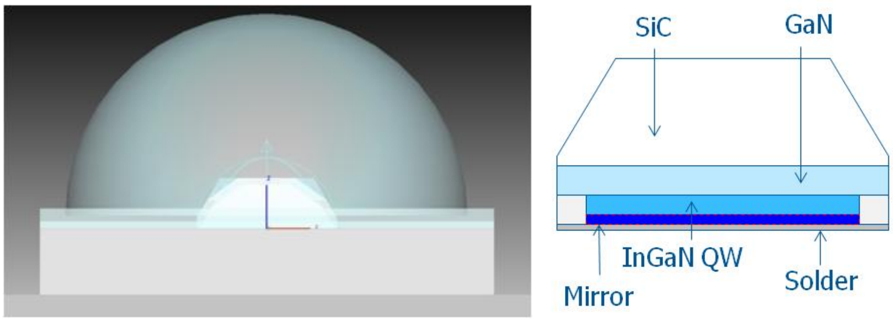

Fig. 2. Schematics of the Cree XT-E package (left) and the DA-1000 chip (right) used in ray tracing simulations to determine the effect of elevated encapsulant RI on white light luminous flux enhancement. The phosphor layer which coats the DA chip is not shown.

To motivate this work, we conducted detailed 3-D ray-tracing simulations to predict the enhancement in LEE at elevated encapsulant RI for a representative Cree chip and package (see Fig. 2). Specifically, we investigated the effect of raising the RI of the encapsulant to establish the effect of this enhanced RI on overall white light luminous flux (see Fig. 3). We used established values for phosphor conversion efficiency, particle size distribution, index of refraction, scattering characteristics, loading, and layer thickness.

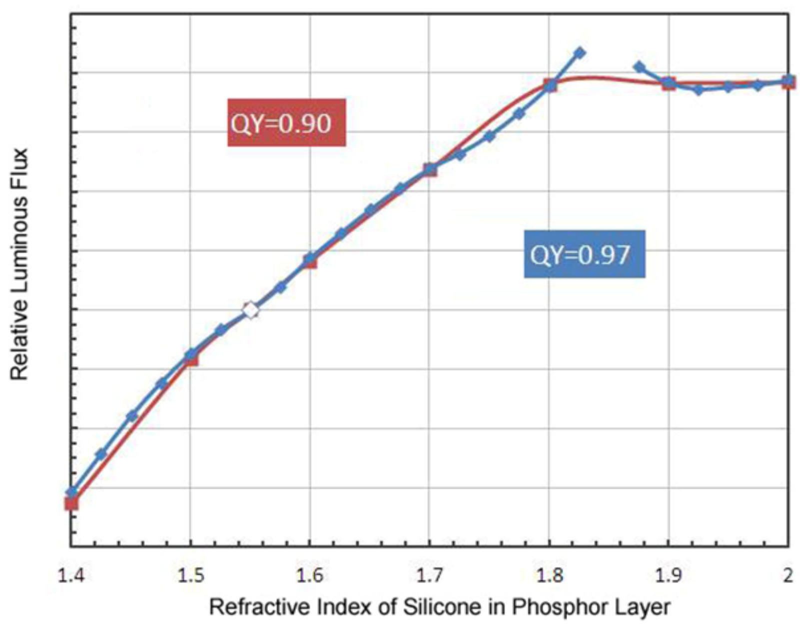

Fig. 3. Simulated relative luminous flux of a warm-white (v' = 0.52) LED vs. RI of the silicone encapsulant, with n = 1.55 as the baseline case (white diamond). Two phosphor quantum yield values are shown, which do not significantly affect the white light relative luminous flux. The discontinuity of the QY=0.97 case at n ~ 1.85 is a modeling artifact and was found to not affect the overall trend.

We also investigated the effect of phosphor layer thickness (and therefore color point) on expected LF gain with increasing RI. As plotted in Fig. 4, the luminous flux tends to increase monotonically as v' increases, with a slope that is fairly independent of silicone RI except at very high v' values. In a manner analogous to the trend in Fig. 3, the net expected LF at all color points increased with silicone RI, but the incremental gain became progressively lower beyond RI ~ 1.8. This initial LED modeling provided us with guidelines as to the composite RI we should be targeting, and the expected LF gains we should observe at various color points.

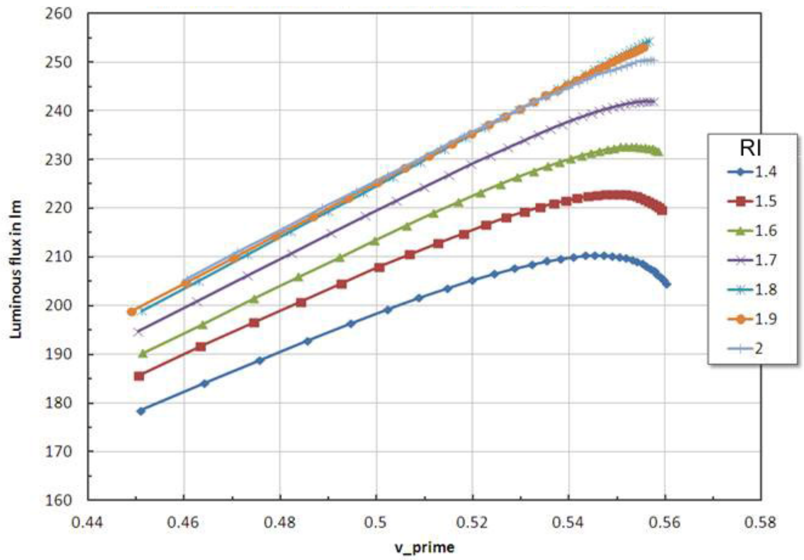

Fig. 4. Simulated luminous flux vs. v' color coordinate at various silicone RI values. The v' range shown corresponds to a phosphor layer thickness range of approximately 50-200µm.

Optimal dispersion of a high-RI phase in the silicone matrix often required modification of the silicone itself. Otherwise, optical clarity was lost due to agglomeration or other effects. This strategy enabled the high-RI phase to be more evenly distributed after silicone curing. We adopted the designation Ix-Cy, indicating the high-RI phase and additive type, respectively.

In Fig. 5 a series of high-RI phases blended in silicone at various concentrations and processing conditions are shown. It is apparent that the optical clarity of the composite was highly dependent on both parameters. At the highest concentration cracking and spalling occurred, indicating that the mechanical properties of the composite were not suitable. At intermediate weight loadings the reaction of the high-RI phase with the silicone was beneficial to clarity, but it could not be carried out in such a way that gelling occurred prior to curing. The transmission at 450nm of the composites was measured with a spectrophotometer, and the values generally agreed with the qualitative assessments made using the photographs in Fig. 5.

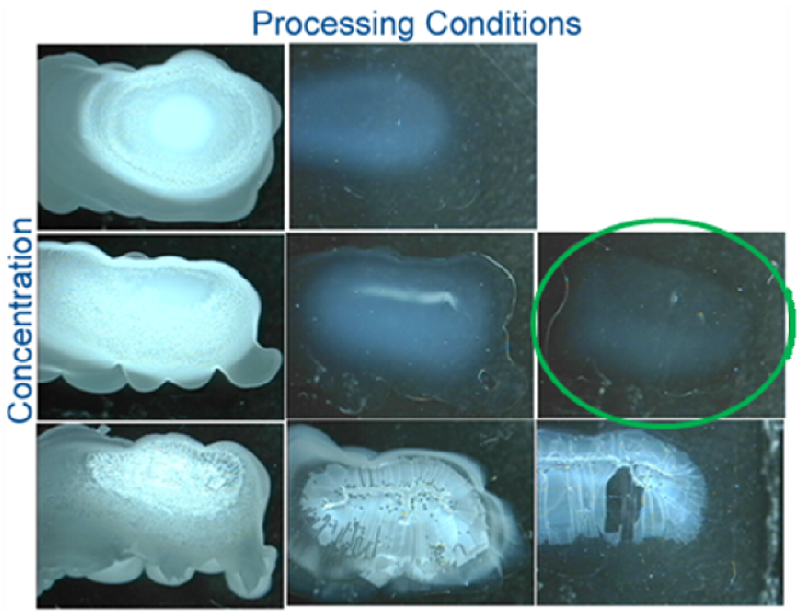

Fig. 5. Photographs of high RI silicone blends at various concentrations (rows) and processing conditions (columns). Composite optical clarity is highly dependent on both parameters.

We incorporated high-RI composites into representative LED packages, using conditions analagous to those in production. An increase of refractive index for this layer should directly increase normalized LED luminous flux (LF). To verify LF differences between these layers and control LEDs, we first measured the radiant flux of all unencapsulated blue chips on the LED panel. We then normalized white LED LF values by these blue radiant flux values to account for chip-to-chip variation.

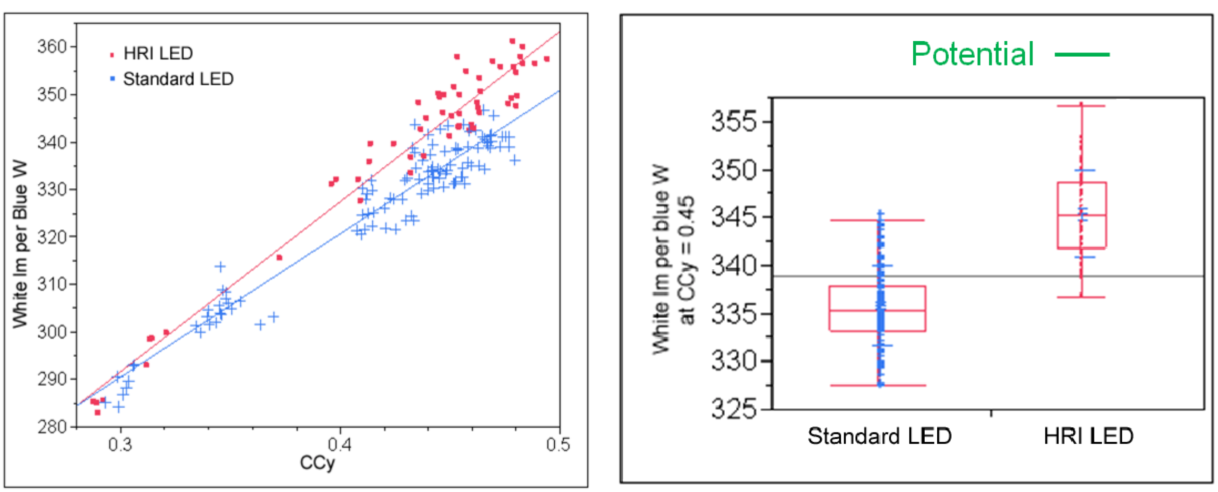

Fig. 6. Left: White LED luminous flux normalized by blue chip radiant flux vs. CC_y color point. Right: All values at left normalized to a single color point (CC_y = 0.45). A statistically significant improvement in LF was observed when utilizing a particle-silicone composite, attributable to its increased refractive index. The maximum calculated potential increase in normalized luminous flux is indicated with a green line.

The LEDs were intentionally fabricated such that a range of color point values were obtained, in order to reveal any luminous flux gain dependence on color point. As shown in Fig. 6, we found that an intermediate concentration resulted in a statistically significant LF increase of >3%, consistent with earlier measurements on high-RI silicone mixtures. Although lower than the predicted value of ~5% at this particle loading, this gain justified further formulation and process experimentation, as well as reliability (accelerated lifetime) testing to determine if the composites were robust at elevated temperature and optical flux.

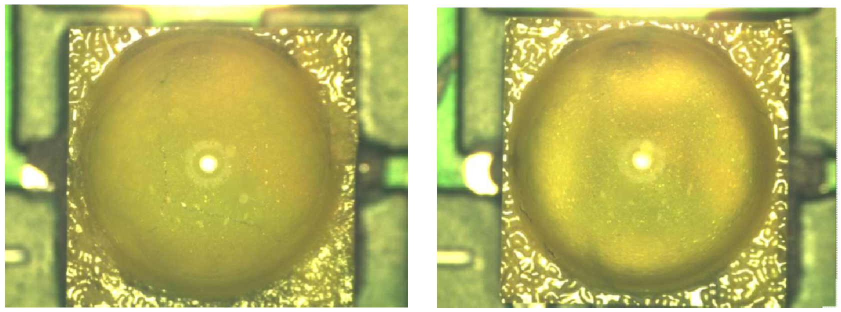

Fig. 7. Left: micrograph of LED with the high-index composite that exhibited cracking after solder reflow. Right: a silicone-only control sample which did not crack.

We began high-temperature/high-humidity accelerated ("reliability") testing of fully fabricated LEDs that incorporated the high-RI composites. This required soldering of fully fabricated LEDs onto circuit boards to enable current flow during exposure to high temperature and/or high humidity inside the test chambers. We observed that for some composites, the solder reflow temperature cycling caused visible cracking (see Fig. 7 left), presumably due to the reduced mechanical compliance of the composite compared to silicone only (Fig. 7 right). Likewise, cracking could also occur during the accelerated testing itself.

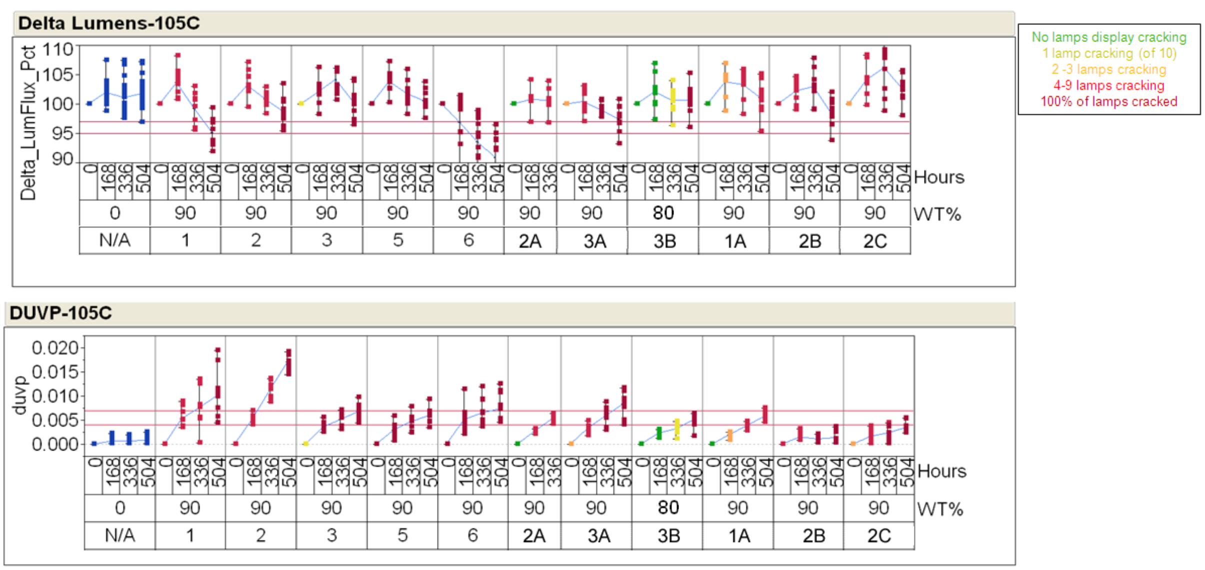

Fig. 8. Luminous flux (top) and color point (bottom) changes during high-temperature accelerated testing of LEDs with high-RI silicone composites. Data points are color-coded to indicate the number of LEDs with visible cracking at each sample time.

The precise implication of such cracking for LED lifetime is not known, but cracking may lead to the luminous flux and color point shifts that are observed during accelerated testing (see Fig. 8). In addition to tracking LF and color point shifts vs. time in the testing conditions, we also counted the number of cracks visible at each sampling point. While cracking could clearly be correlated with color shifts for some samples, others exhibited color shift *before* cracking was detected. Further trials were conducted to determine LED processing conditions under which cracking can be avoided, and also to gain a better understanding of the source of the LF and color point shifts shown in Fig. 8.

As shown in Fig. 9, it is evident that a du'v' color shift of some LEDs set in before cracking was observed. Thus there could be one or more mechanisms responsible for color point shifts that are independent of those responsible for cracking. One likely candidate is the thermal and/or optical stability of the high-RI phase as dispersed in the silicone matrix. We investigated chemical variations in this phase which would result in minimal color shifting in accelerated testing conditions, while at the same time reducing or eliminating the likelihood of cracking during this testing.

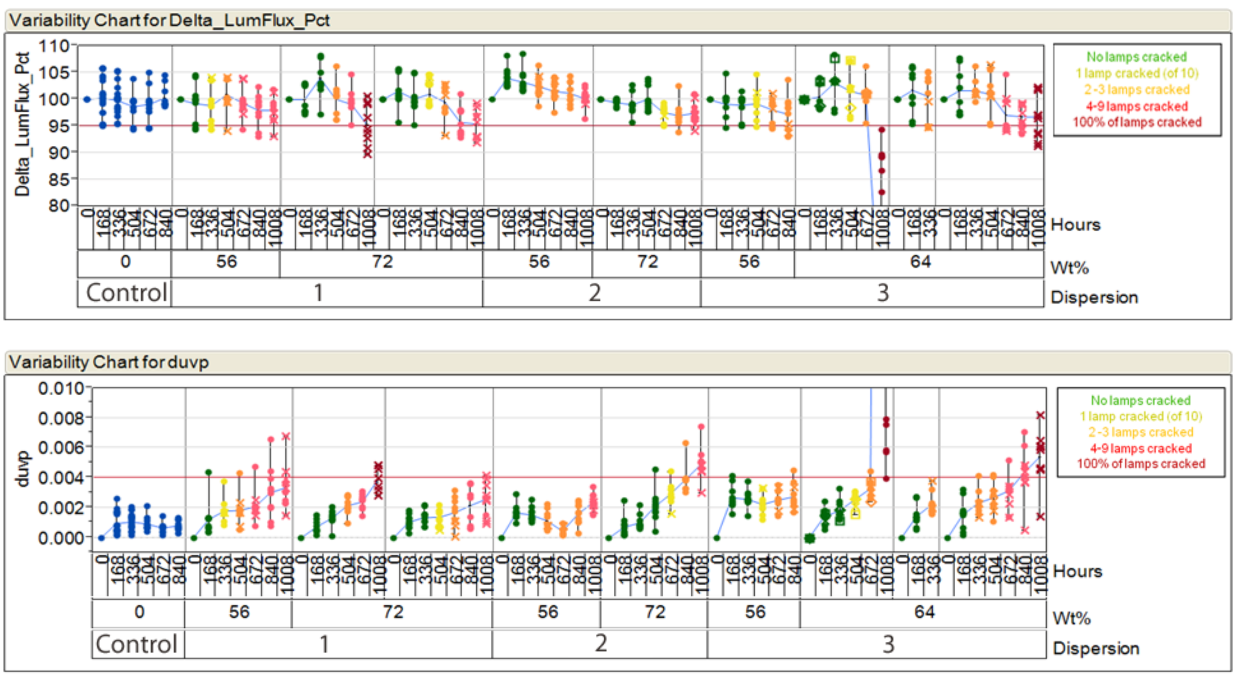

Fig. 9. Luminous flux change (top) and color point shift (bottom) of prototype LEDs containing high-RI silicone composites. The color point of some LEDs (*e.g.* dispersion 2 with 72 wt% particles) shifted prior to the onset of significant cracking.

Later work on high-RI silicone composites focused on the modification of the silicone matrix to lower its starting hardness, in order to correspondingly lower the composite hardness. This was found to be beneficial to not only as-fabricated LED mechanical properties, but also to the lumen maintenance and color shifting characteristics of prototype LEDs during accelerated testing (reliability) at elevated temperature, light flux, and/or humidity. Although visual cracking was often, though not always, associated with luminous flux and color shifts, we conservatively viewed cracking in any form to be unacceptable for products, as its long-term effects on overall LED reliability were unknown.

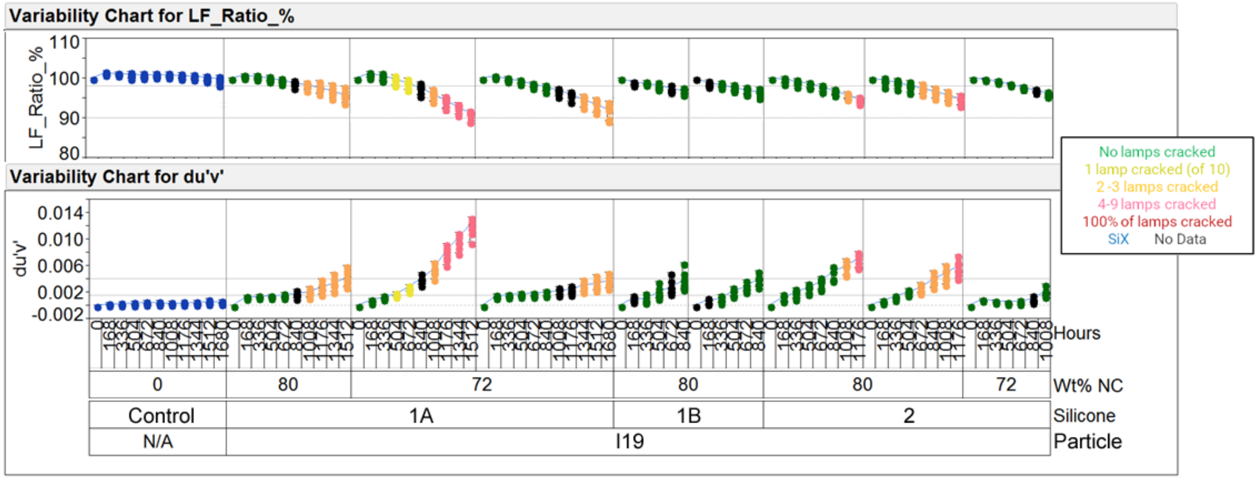

Fig. 10. Luminous flux (top) and color point (bottom) shifts vs. time in high-temperature LED accelerated testing for prototype LEDs containing high-RI composites. The formulation at far right (formulation I19 in Silicone 2) passed the 1,000 hr. reliability milestone due on 7/31/15.

In a variation of the blending approach described above, we utilized softer silicone formulations which were based on standard formulations with well-characterized high-temperature/high-flux stability. The resulting silicone-particle composite hardness thus of a level which enabled more compliance with mechanical stresses that develop in LEDs at high temperature. Reliability testing revealed promising indications for high-T/high-flux stability of a few of these composites, as shown in Fig. 10. At >1,000 hrs. under the accelerated testing conditions we were employing, the average luminous flux and color point shifts of several LED types containing high-RI composites was within acceptable ranges (<10% LF, <0.004 du'v'). In fact, one formulation (I19 particles in Silicone 2, see Fig. 10 far right) passed the 1,000 hr. reliability milestone of <10% LF drop. However, we note that for other formulations some cracking was still observed, as indicated by the orange and pink points. We continued testing these samples to determine if LF and color point shifts set in after this initial period. In addition, we planned to further modify the softer silicones with organic species of lower molecular weight than the host silicone backbone, in an effort to produce further mechanical compliance under high-T/high-flux conditions.

Early studies indicated that when LED packages with composite encapsulants were subjected to solder reflow testing (a temperature excursion to ~260°C for ~30 seconds), their luminous flux and/or color point could be altered. An example is shown in Fig. 11, in which the luminous flux of HRI LEDs degraded by ~1.7% after a 3x reflow cycling test.

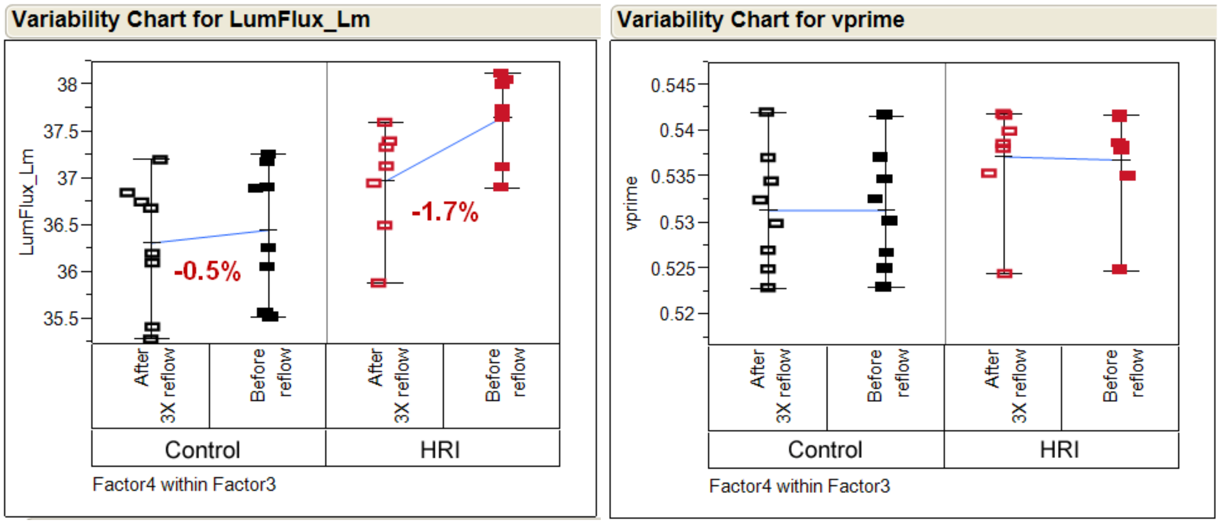

Fig. 11. Luminous flux (left) and color points (right) of HRI and control filled-lens LEDs before and after 3x solder reflow temperature cycling. The luminous flux of the HRI LEDs degraded after being subjected to this condition.

Via optimization of the process steps used to blend the high-RI phase into the silicone matrix (without also detrimentally affecting the blending of the phosphor into the silicone) and modifications to the silicone matrix to reduce post-cure hardness, we were able to mitigate the luminous flux degradation observed in reflow. The data in Fig. 12 indicate that after these process improvements, HRI LEDs had nearly the same negligible luminous flux drop and color shift as control LEDs of this type.

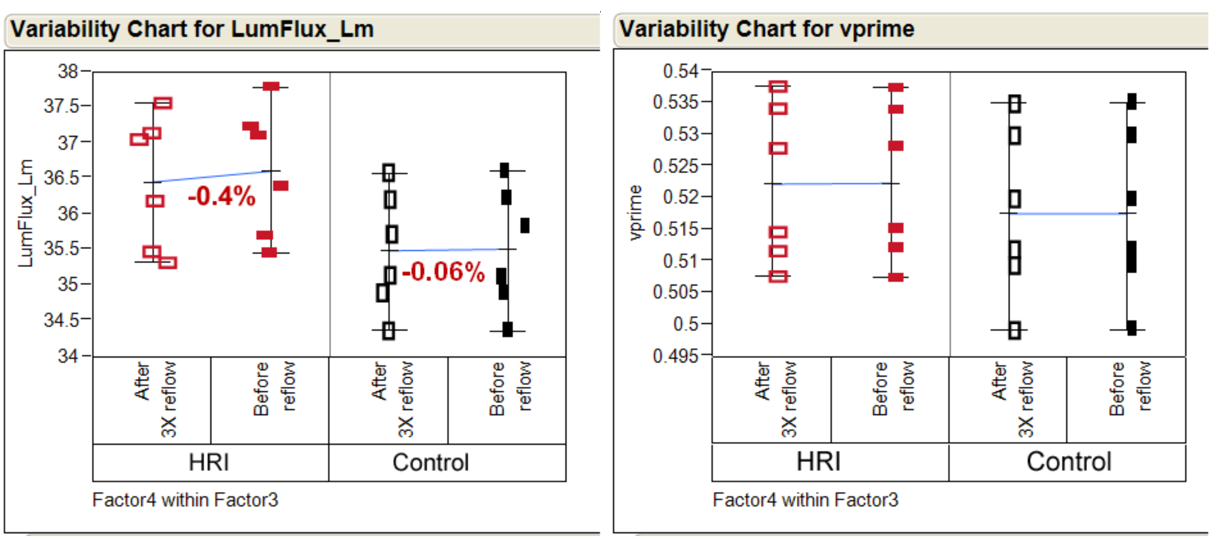

Fig. 12. Luminous flux (left) and color points (right) of HRI and control filled-lens LEDs before and after 3x solder reflow temperature cycling, after process improvements and silicone matrix modifications.

The results above focused on the simplified case of LEDs with blue chip + green/yellow phosphor, with resulting color points along a tie line off of the blackbody locus (BBL) in the CIE x-y color diagram. Later we also explored the more challenging case of warm-white color points on or near the BBL by including red phosphors. An example is shown in Fig. 13, in which color points of numerous prototype warm-white LEDs are plotted, which verified that they lay in close enough proximity to make valid luminous flux (or efficacy) comparisons. Likewise, their color rendering index (CRI) values were all within 1-2 points, obviating the need for corrections due to CRI disparity.

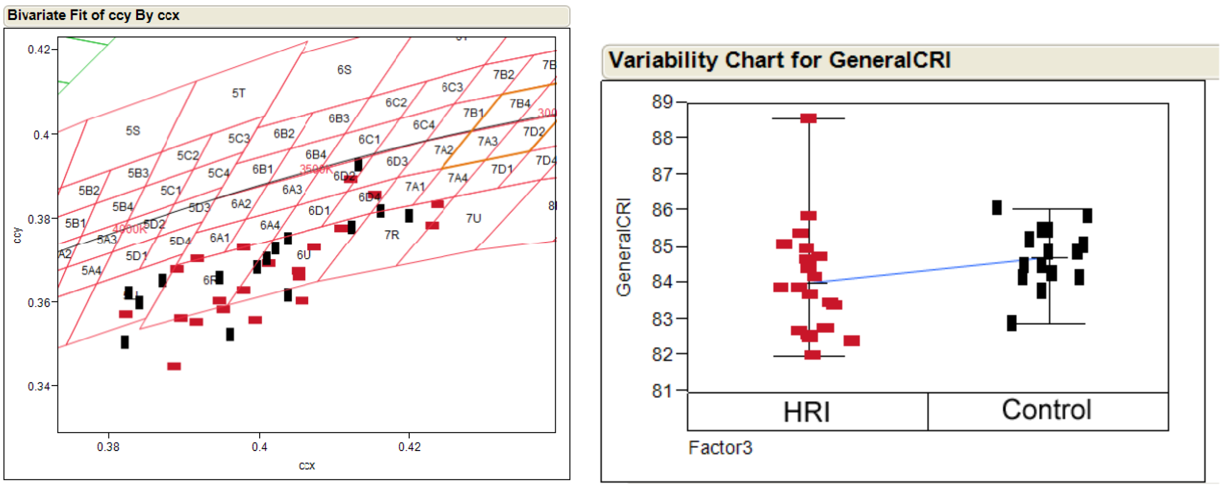

Fig. 13. Left: color points of control (black) and HRI prototype LEDs (red) in CIE x,y color space, indicating their proximity to ~3500K. Right: Color Rendering Index (CRI) of HRI vs. control warm-white LEDs.

The normalized luminous flux of the HRI vs. control warm-white LED packages was measured by first quantifying the blue light flux emitted by each package, and then measuring the white light luminous flux mapped over the same packages. This "leveled the playing field" and reduced uncertainty in luminous flux among packages that might have arisen due to variations in blue chip flux. As shown in Fig. 14, incorporation of high-index inorganic particles in the HRI warm-white LEDs led to an increase of 2.5% over the control case, which is similar to the off-BBL results above.

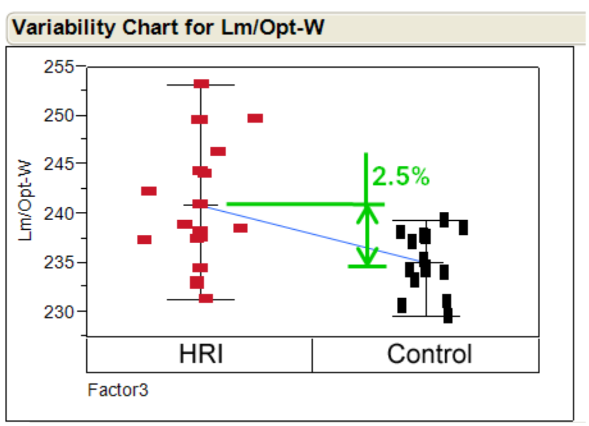

Fig. 14. Normalized luminous flux of HRI vs. control warm-white LEDs, indicating an average gain of 2.5% due to HRI.

High-Efficacy TrueWhite components

Early efforts at increasing the efficacy of LEDs with high color quality focused on the integrated TrueWhite® approach, which combined yellow/green phosphor-coated blue chips with red chips in the same package. Implementing the TrueWhite approach within a single LED package presented challenges such as far-field color uniformity and potential absorption of blue, green, and yellow light by the red chips. We designed and fabricated several different chip configurations consisting of varying numbers and positions of blue and red chips. To accurately target a color temperature of 3000K on the black-body locus, the luminous flux (LF) vs. current was independently measured for the blue+phosphor vs. red chips, as shown in Fig. 15.

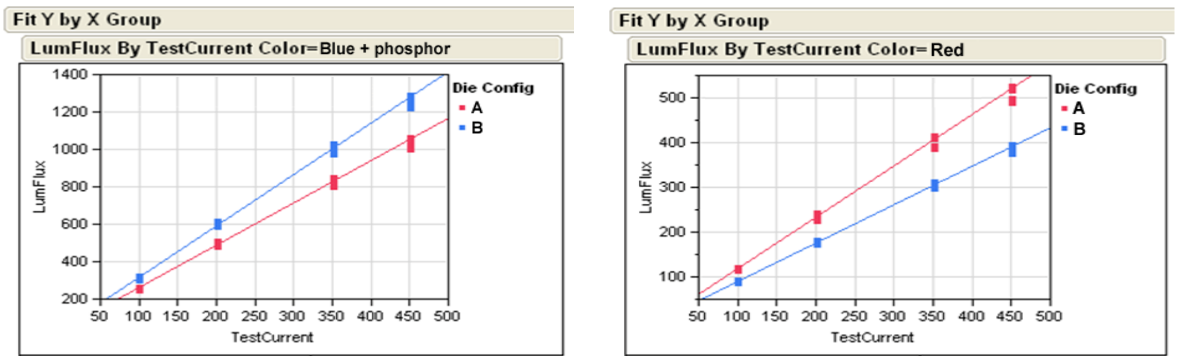

Fig. 15. Instant-on luminous flux vs. drive current measured for the blue+phosphor (left) and red (right) chips in two integrated TrueWhite packages with differing chip configurations (A,B). Configuration A had superior LF at all drive current values.

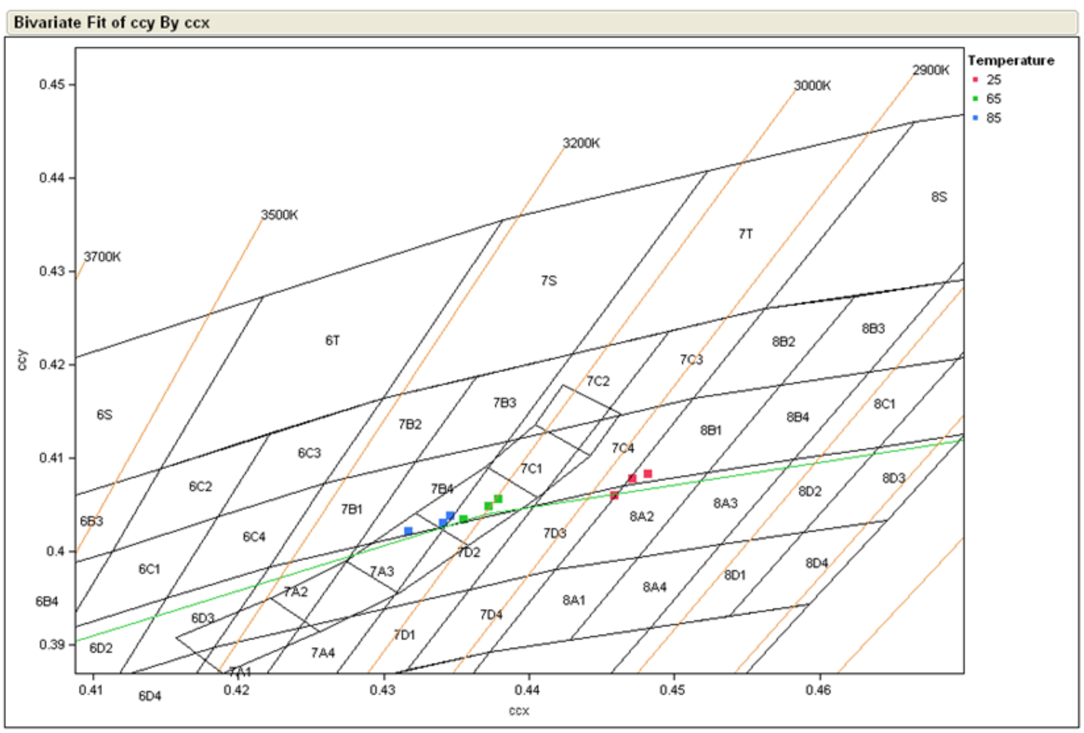

Fig. 16. CIE color coordinates of integrated TrueWhite configuration A vs. nominal operating temperature. The color temperature increased with operating temperature, but all color points fell on or near the black-body locus.

By independently assessing the LF of the two LED strings, we targeted a color temperature of ~3000K on the black-body locus (see Fig. 16) by varying the blue and red chip currents. At this color point, the average room-temperature, “instant on” package efficacy was **~145 lm/W** at a package power density of ~1 W/mm^2. We designated this power density as a baseline that as equivalent to the DOE-designated current density baseline of 35 A/cm^2 (since, for a 1mm x 1mm blue chip as originally envisioned by DOE, 35 A/cm^2 ~ 1 W/mm^2). This was done due to the difficulty of stating an ‘average’ current density when both blue and red chips were used, since they were driven independently of each other.

The color point, efficacy, and CRI values of package configuration A were measured under “instant on” conditions at room temperature, 65°C, and 85°C to establish their temperature dependence for eventual operation under ‘realistic’ system thermal conditions. As shown in Fig. 17, the color point shifted to slightly longer CCT values but did not depart significantly from the black-body locus. Package efficacy decreased linearly with temperature (Fig. 17 left) as expected, while the CRI increased (Fig. 17 right). This is apparently due to slight shifting of the red chip peak wavelength (from shorter to longer) over this temperature span.

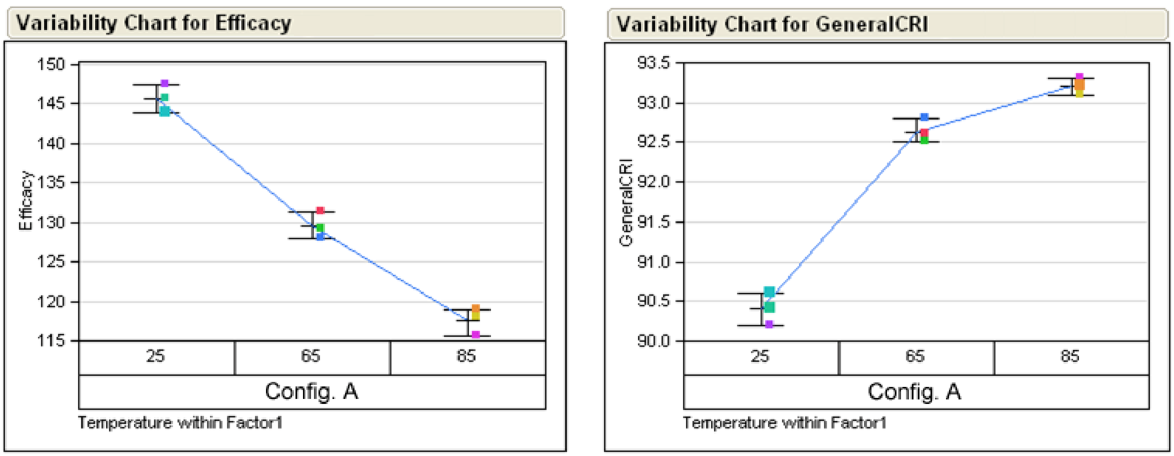

Fig. 17. Instant-on integrated TrueWhite® package efficacy (left) and CRI (right) at room temperature, 65°C, and 85°C. As expected, the efficacy fell roughly linearly with temperature, while the CRI increased, nominally due to slight spectral shifts (primarily in red peak wavelength).

Principal challenges in the integrated TrueWhite® approach included: selective phosphor application on blue chips; far-field emission color uniformity; and potential absorption of blue, green, and yellow light by the red chips. The first of these challenges, phosphor selectivity, was studied for a number of fabrication runs by quantifying the color point variability from run to run. This variability should have been low if the selective application process avoided coating red-emitting chips with yellow/green downconverters, and also resulted in consistent downconverter coverage on the package floor. With one exception, this was found to be the case over eight successive runs, where the v’ color coordinate was measured for numerous devices on each panel. As shown in Fig. 18, the standard deviation (σ) in v’ coordinate was 0.001 to 0.002, on par with the control (standard domed phosphor-only) packages. Thus the full distribution ($\pm 3\sigma$) width would be less than **0.006 in v’**, which satisfied our milestone target of < 0.007 variation and indicated the practicality of this package architecture for volume production.

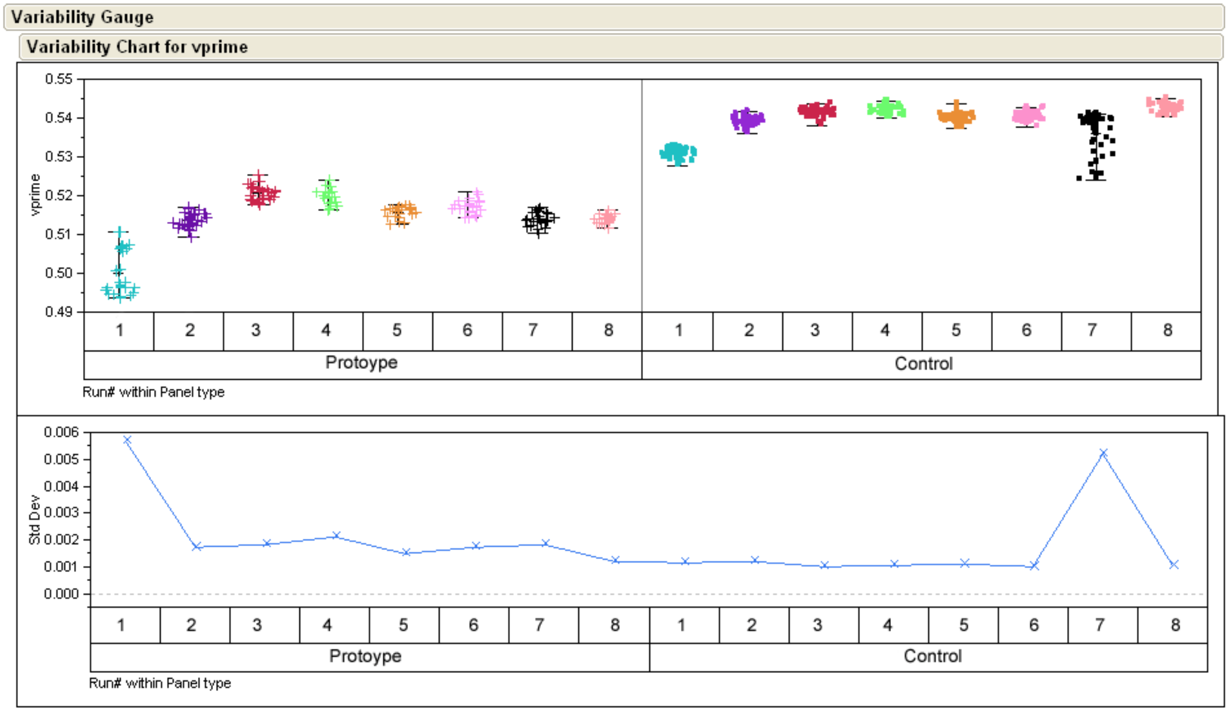

Fig. 18. Variation in v' color coordinate over eight runs for prototype packages (left) compared to standard all-phosphor domed components (right). With one exception for each type, the standard deviation in both cases was 0.001 to 0.002, indicating high color point reproducibility.

As for all prototype LED designs, the reliability (accelerated lifetime) characteristics of numerous sets of integrated TrueWhite LED packages were evaluated in Cree's standard high-temperature, high- humidity accelerated testing conditions to verify that this design did not introduce any new failure mechanisms. As shown in Fig. 19, the luminous flux of the blue+yellow and red strings was evaluated independently to best elucidate the sources of any undesirable changes. For numerous sets of prototype packages, the relative luminous flux of both strings was acceptable for periods of up to 3,024 hrs., with the red chips typically exhibiting more degradation but still staying within the -10% acceptability criterion. We therefore met the 1,000 hr. reliability milestone for Month 12.

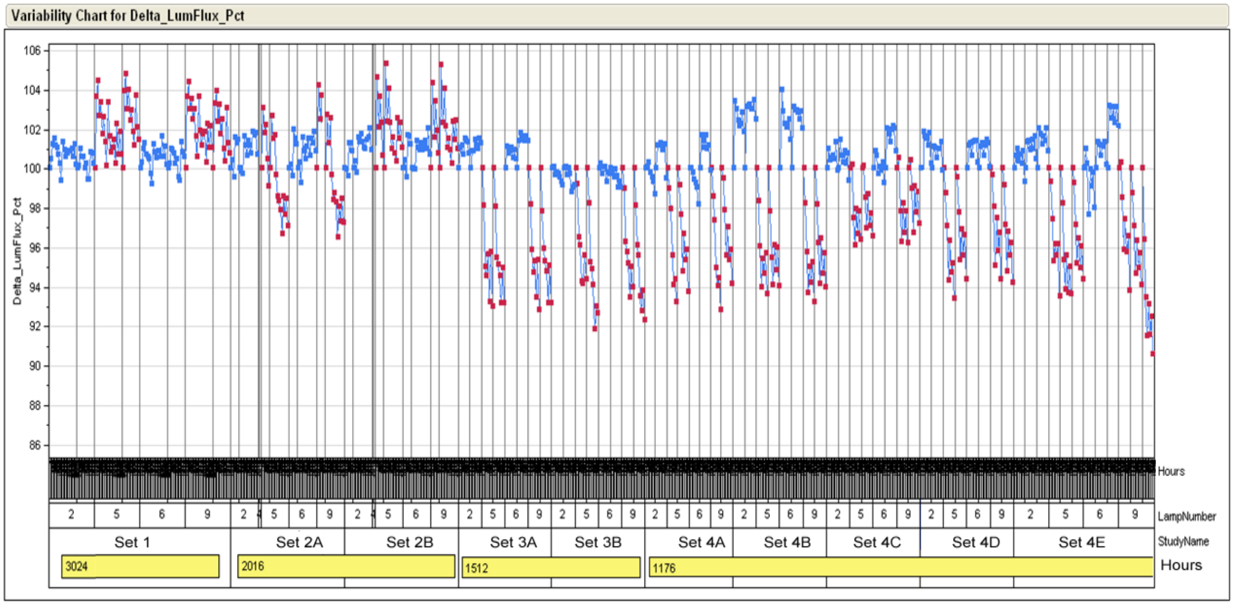

Fig. 19. Luminous flux changes during reliability testing of numerous integrated TrueWhite configurations.

Narrow-band Downconverters

In the effort to increase the efficacy of warm-white LEDs with high color quality, we modeled and fabricated mixtures of yellow-green phosphors and red narrow-band down-converters, which offer higher spectral efficiency than conventional red phosphors when utilized in the same LED package footprint. This approach also has the advantage over hybrid schemes such as TrueWhite® of lower system-level optical mixing requirements, and lower driver complexity since one string (circuit) is needed instead of two or more. LEDs with the phosphor-NBD formulation in Fig. 20 exhibited an "instant on" efficacy of 151 lm/W at ~3000K and ~83 CRI when driven at the DOE baseline current density of 35 A/cm^2 at room temperature.

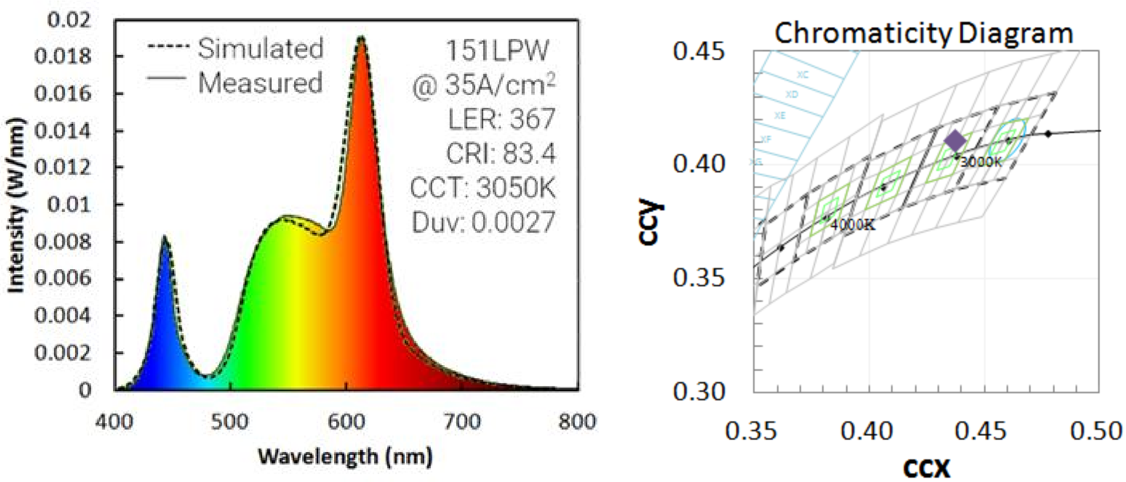

Fig. 20. Left: measured vs. simulated spectra for a prototype LED containing narrow-band downconverters, accompanied by key performance characteristics. Right: color point of this LED plotted on the CIE x-y diagram, indicated its proximity to the BBL at ~3000K.

Via comparison of simulated vs. measured spectra and efficacy values, we identified areas for further improvement (such as is being pursued in the newer DE-EE0007079 program). As shown in Fig. 21, the position of the narrow (~35nm) red emission peak is a key "lever" in balancing the tradeoff between efficacy and CRI. While the CRI reaches a maximum at a peak wavelength of ~622nm, the net efficacy (*i.e.* including package losses) monotonically decreases as red peak wavelength increases. This is due to the decreasing net luminous efficacy of radiation (LER) which results from progressively moving the red peak outside the envelope of the human eye response curve. Thus to achieve ~90 CRI at ~622nm, some efficacy loss will be observed compared to what could be achieved at ~600nm, for example. To align the simulated efficacy with the measured value, we estimated a package loss of ~10% for this un-optimized geometry, which could be lowered to ~5% with more reflective surfaces. In addition, we planned to employ narrower green phosphors to improve LER, but the quantum yield of these phosphors must nearly match that of the yellow-green blend used in this case.

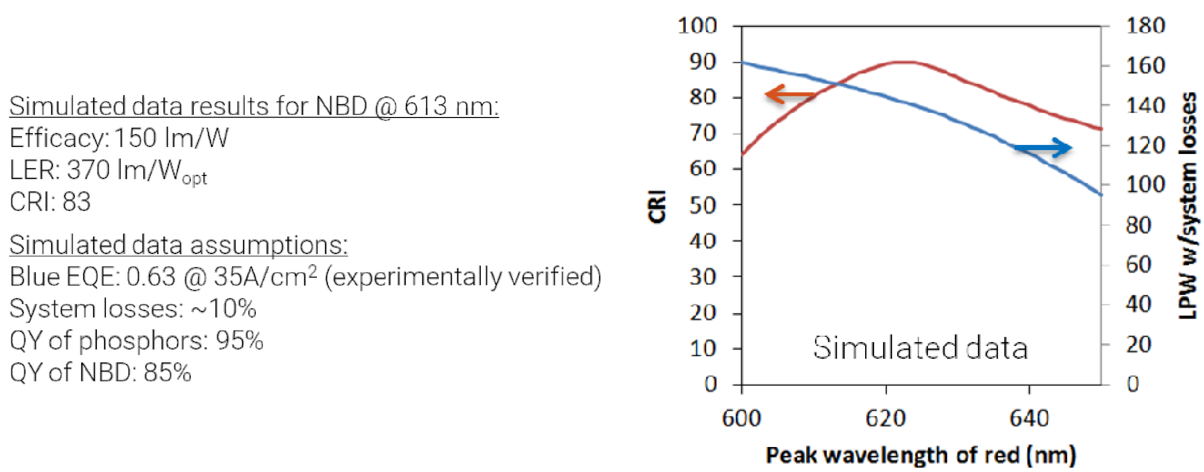

Fig. 21. Left: Simulated data results and assumptions used in analyzing the measured spectrum in Fig. 20. Right: the simulated dependence of CRI and efficacy on red peak wavelength, indicating the tradeoff among these two characteristics.

Task 3: Light Module Design, Testing

As described above, integrated TrueWhite® LEDs provide a route to simultaneously high efficacy and color rendering index. However, they also present the challenge of uniform far-field color mixing, which is largely dependent on package lens geometry. In addition, color mixing can be managed via the optical design of the lightguide coupling cavity. We simulated TrueWhite LEDs in a simplified cylindrical lightguide coupling cavity, as well as an optimized cavity whose shape had been designed to provide for enhanced color mixing within the lightguide. In Fig. 22 it is evident that while there were still some perceptible color point variations in the optimized case, they were minor and could likely be further mitigated with the use of a light diffuser over the lightguide. This comparison illustrated the need for LED package and coupling cavity optical designs which are developed synergistically to fully exploit the potential use of integrated TrueWhite packages in the Light Module.

Although color uniformity may be challenging when using integrated TrueWhite® LEDs, even with conventional phosphor-converted LED packages color mixing over progressively larger lightguide areas can be lower than desired. We investigated the effect of all-phosphor LED color binning on module color point variation, since a large color point disparity between nearest neighbors could cause unacceptable observed color differences over several Light Module 'unit cells'. Via measurements and simulations we gained a better understanding of the sensitivity of the viewer to LED-to-LED color point variation, and therefore the amount of "allowable" variation in production. This may eventually dictate how tightly the LEDs need to be binned in color space (and/or luminous flux) when used in such low-profile Light Modules.

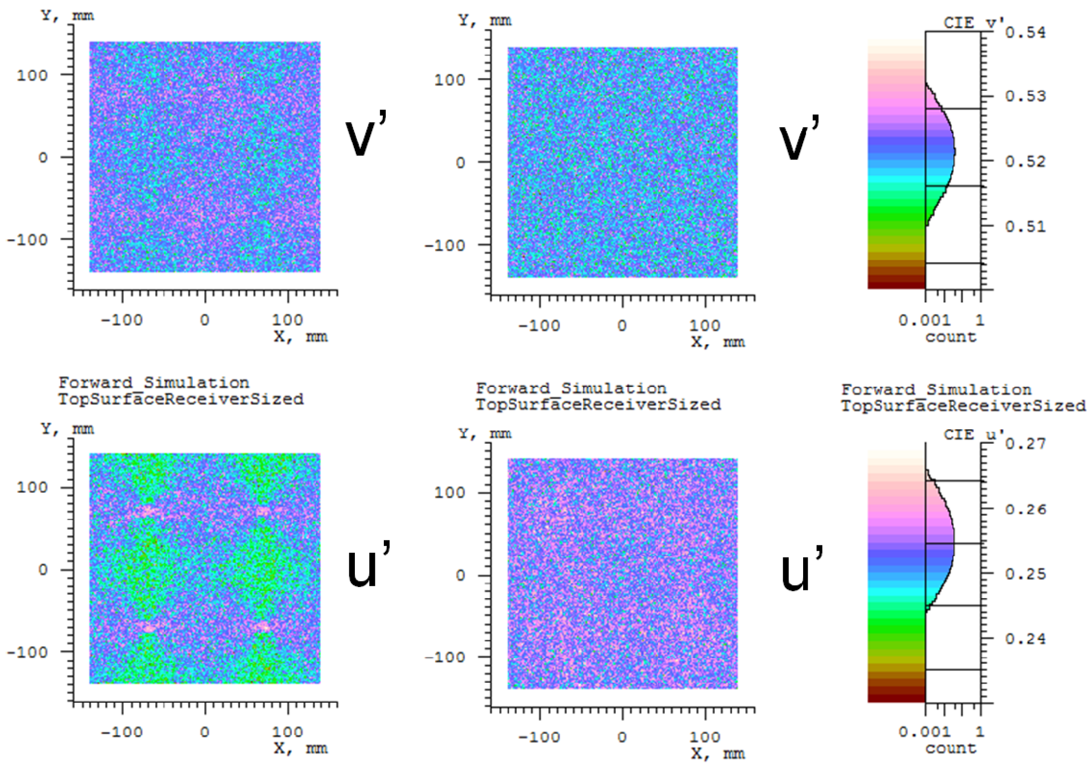

Fig. 22. Simulated color point coordinate variation over a 1x1 ft. low-profile module with a TrueWhite LED in a simple cylindrical cavity (left) and more complex optimized cavity (right). The color point uniformity is much lower for the former, since no efforts were made to effectively blend light within the lightguide prior to extraction.

An example of color point difference evaluation is shown in Fig. 23, in which 12"x12" Light Module was analyzed using an imaging colorimeter with a 16 bit CCD and 1024x1024 pixel array. The u', v', and combined u'v' color point values were recorded using a module with LEDs in the left half intentionally separated by two color bins from those in the right half. By correlating these measurements with visual observations, we found that a two-bin color point separation was tolerable. As such, this conditionally places an upper limit on the tolerable LED color point variation when using this module design. Lightguide extraction schemes which encourage more light intermixing between neighboring cells are under consideration, with the goal of not sacrificing overall optical efficiency.

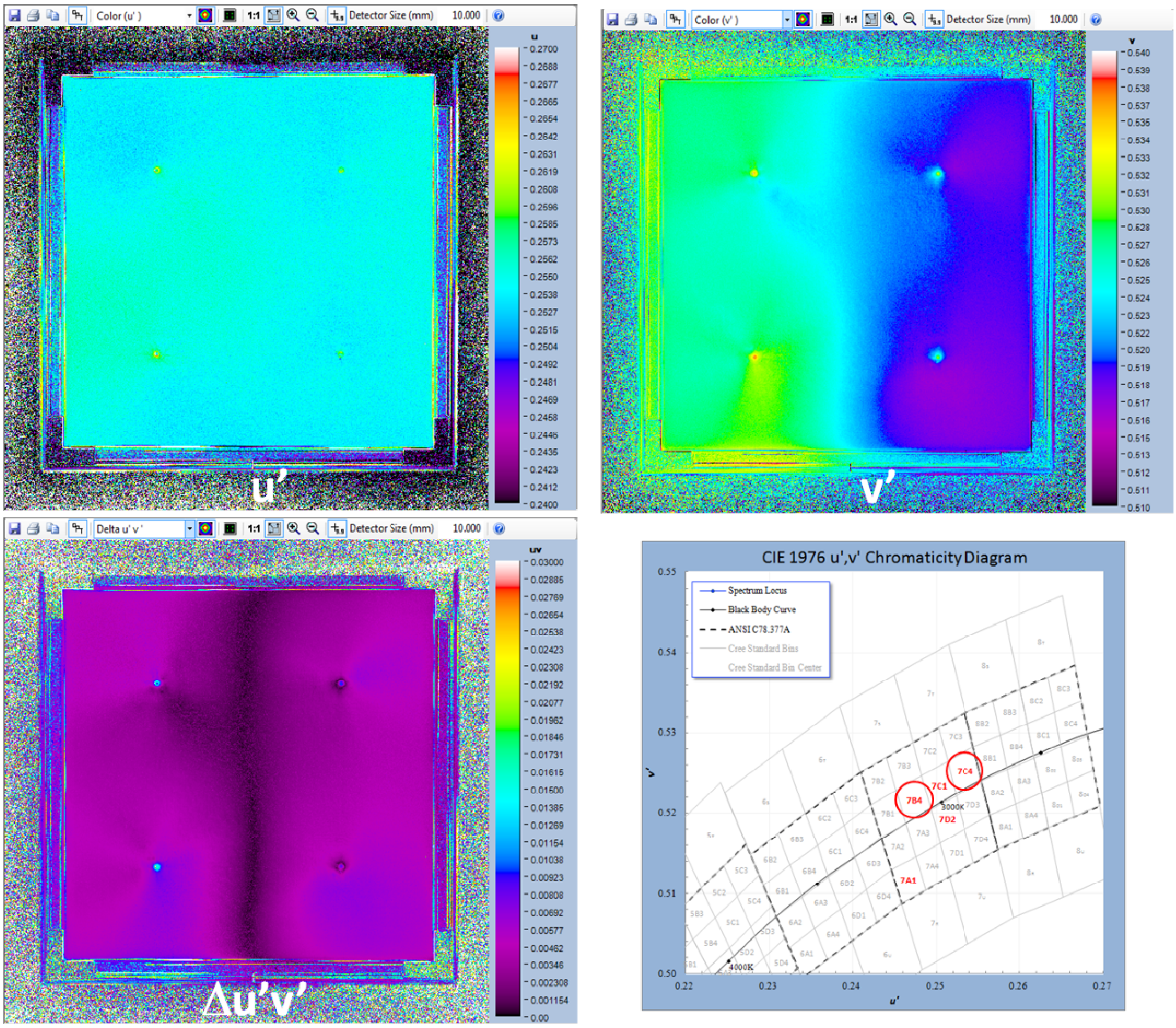

Fig. 23. Imaging colorimeter scans of a 12”x12” light module having LEDs on the left and right separated by two color bins. The upper plots show u’ and v’ vs. position, while the lower left plot combines u’ and v’ together. The bin locations in color space are shown at lower right. Such data, in combination with visual observations, indicated that the difference in v’ color coordinate was more perceptible than u’.

We evaluated the emission characteristics of several prototype Light Module designs of 6x6” and 12”x12” size, primarily via colorimeter imaging but also via integrating sphere measurements which indicated the optical efficiency of each design. An example is shown in Fig. 24, in which only the LEDs in a prototype module were first measured, and then the lightguide and extraction optics were overlaid to quantify the degree of light loss. Even with a diffuser in place to provide enhanced luminance uniformity (with accompanying scattering losses), an optical efficiency of ~94% was reached. In general we pursued Light Module designs in which a diffuser would not be ultimately necessary, which would lower materials and assembly costs, as well as provide for higher system optical efficiency.

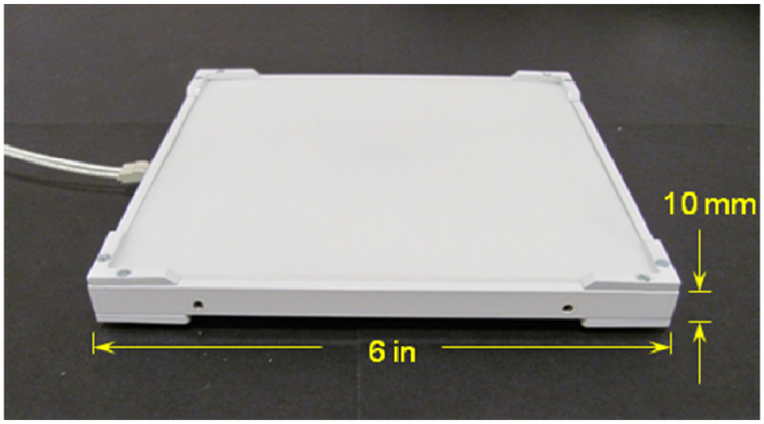

	Description	LumFlux lm	Relative %	u'	v'	CCT K	CRI
No Waveguide	LED only	105.6	100%	0.2570	0.5268	2820	80
Waveguide	Without diffuser	102.5	97.0%	0.2560	0.5267	2843	80
	With diffuser	99.3	94.1%	0.2562	0.5270	2837	80

Fig. 25. Top: photograph of a 6x6" prototype Light Module. Bottom: Luminous flux measurements of this module, indicating a >94% optical efficiency with a diffuser in place over the lightguide and extraction optics.

During Light Module design and testing it became apparent that while LED coupling geometry and dimensional tolerances were important for determining overall optical efficiency, the actual vs. ideal shapes and sizes of the light extraction features on the lightguide surface presented as much (or more) of a challenge for volume production. The most frequently investigated extraction feature geometry consisted of repeated geometrical features inset into the lightguide surface. In speaking to several potential vendors for such patterned acrylic lightguides we learned that injection molding may not be feasible due to the small feature size and/or the tight dimensional tolerances required for a given feature shape. Subsequently, hot embossing became a more likely candidate for defining features over large areas. This process consists of softening the acrylic via heating above its glass transition temperature, and then rolling or pressing a pre-machined form into the surface. When the acrylic cools and the form is removed, the features remain as indicated in Fig. 26. We began evaluating whether this process had` sufficient spatial 'resolution' and reproducibility for subtractive extraction features.

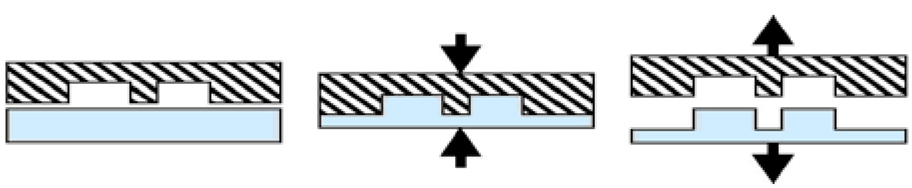

Fig. 26. Schematic of the hot embossing process, in which acrylic is softening and a machined metal surface is pressed into it to define small features.

Early lightguide coupling work largely focused on the use of translucent elements around the LED(s) to help redirect light into the lightguide. Later, a scheme utilizing a specular or

Lambertian coupling cavity reflector was pursued since it was compatible with several candidate wide-area luminaire designs. As shown in Fig. 27 for a specular reflective element, the light from a square-lens component could be efficiently directed into two opposing lightguide surfaces. Various cavity widths (*i.e.* inter-lightguide spacings) and reflector angles were simulated, as depicted in Fig. 27. It appeared that over a wide range of reflector angles, a high (> 90%) lightguide coupling efficiency could be achieved even in the presence of typical printed circuit board (PCB) reflectance of 85-90%. A closer lightguide spacing enhanced the coupling efficiency, which was feasible due to the relatively small size of the LEDs being considered.

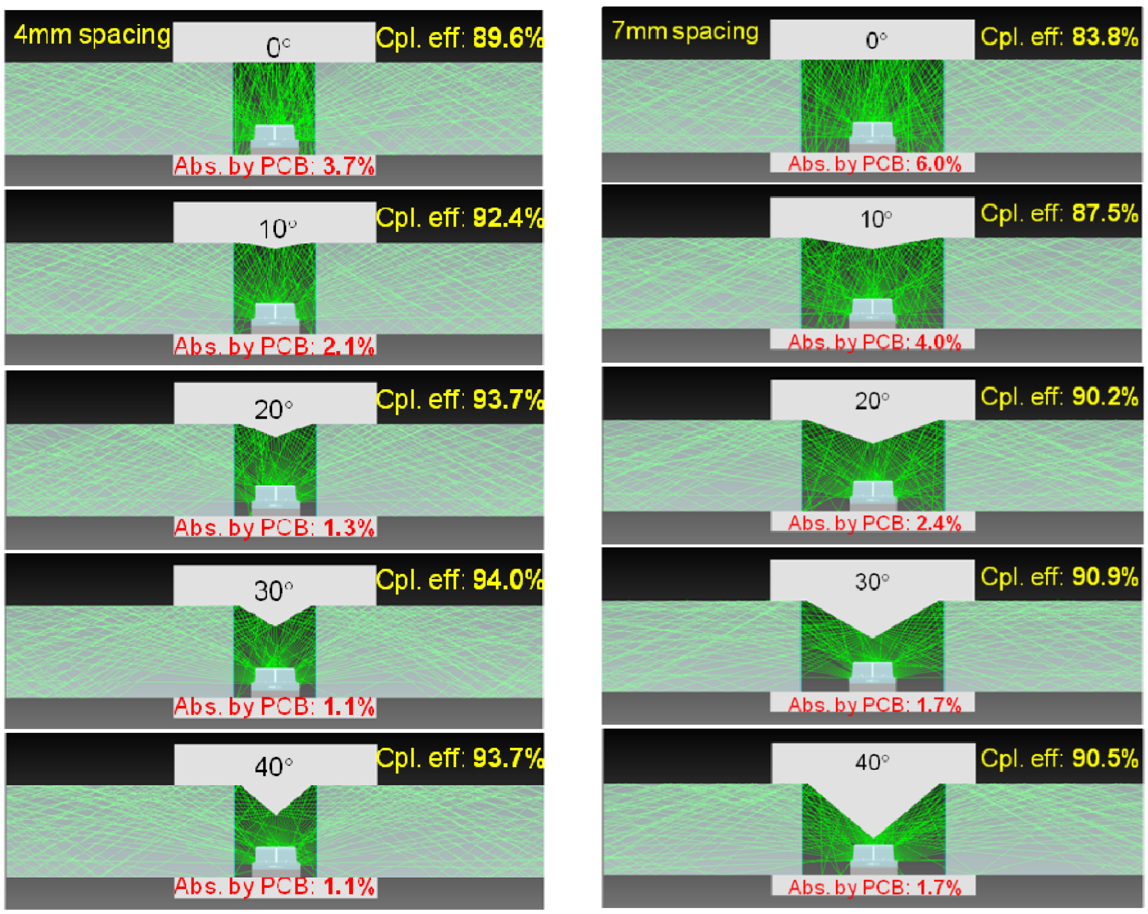

Fig. 27. Ray-tracing simulation of the light coupling from an LED into lightguide edges with two different cavity widths (4 and 7mm) and reflector angles (0-40°).

The LED-to-lightguide coupling efficiency as a function of reflector base angle is summarized in Fig. 28. It was apparent that at nearly all angles, a specular reflector was preferable to a Lambertian one, and also that 4 mm spacing was superior to 7mm. Further optimization studies will consider the effect of the reflector shape as well as LED luminous flux over angle, which is dependent on LED primary optic shape.

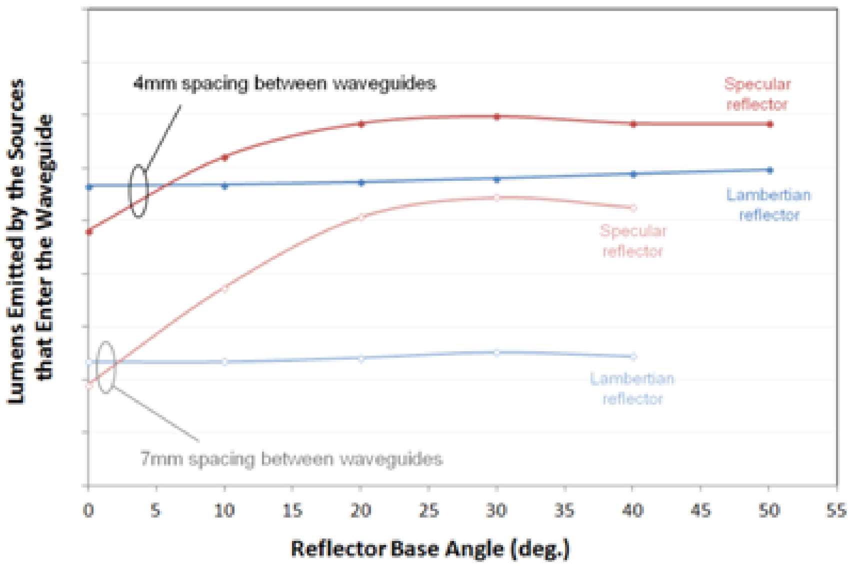

Fig. 28. Coupling efficiency (LED into lightguide) vs. reflector angle for various configurations. The highest coupling efficiency was observed for a specular reflector with 4mm cavity width.

Light Module fabrication work focused on process control of bonding processes joining extraction films to lightguides, as well as the implications of imperfect adhesive profile at the intersections of extraction features and the planar lightguide. Due to the unfamiliarity of this new optical system, we also worked to develop accelerated testing methods which would highlight the strengths and weaknesses of a given extractor film / lightguide / adhesive system. In a manner analogous to LED reliability testing, we chose testing conditions which would accelerate anticipated failure mechanisms while not inducing failure modes which are unlikely to crop up during actual application. To this end, particularly considering the properties of the optically clear adhesives we were evaluating, we chose accelerated testing conditions we termed High Temperature Storage Lifetime (HTSL – 60°C) and Wet High Temperature Storage Lifetime (WHTSL – 60°C / 90% RH). Conditions for Thermal Shock (TS) testing are still being established, and the addition of light to the test samples (which would constitute "High Temperature *Operating* Lifetime", such as for typical LED testing) was planned after the program ended.

As is typically tracked for LED reliability testing, we periodically measured the luminous flux and color point for scaled prototype Light Modules with varying extraction features and adhesives. An example of HTSL testing is shown in Fig. 29, which indicates the stability of optically clear adhesive when exposed to elevated temperature. In this case, the luminous flux did not change appreciably, but the color points of all samples shifted. This indicated that the adhesives may have started degrading (*e.g.* via yellowing), and that if the color point were to continue to shift, the adhesives would have to be rejected. Otherwise, an initial color shift could be acceptable for production if it stabilized and didn't also correspond to significant optical loss.

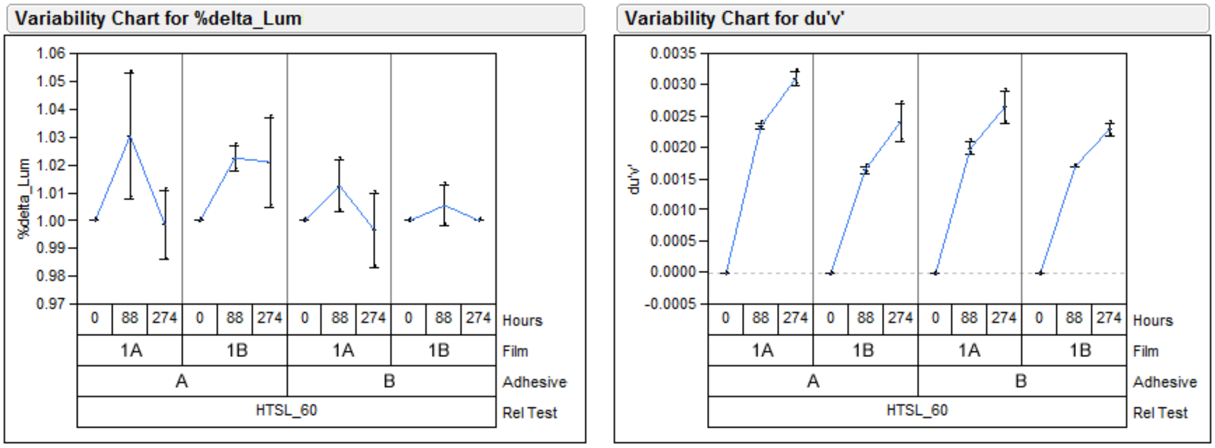

Fig. 29. Luminous flux (left) and color point (right) of adhesive-bonded lightguide-film samples subjected to HTSL testing. Although LF values did not shift appreciably, the color points of all samples changed by more than two steps within 274 hrs.

The more aggressive WHTSL testing typically induced both LF and color point shifts in prototype samples, as shown in Fig. 30. Adhesive B on film 1A in particular showed rapid degradation in LF within 232 hrs., which was found to be due to delamination and is of course unacceptable for consideration in products. Based on these initial results it was anticipated that optically clear adhesives would face challenges in meeting our reliability requirements, whether due to adhesive degradation itself or delamination between the film and the lightguide.

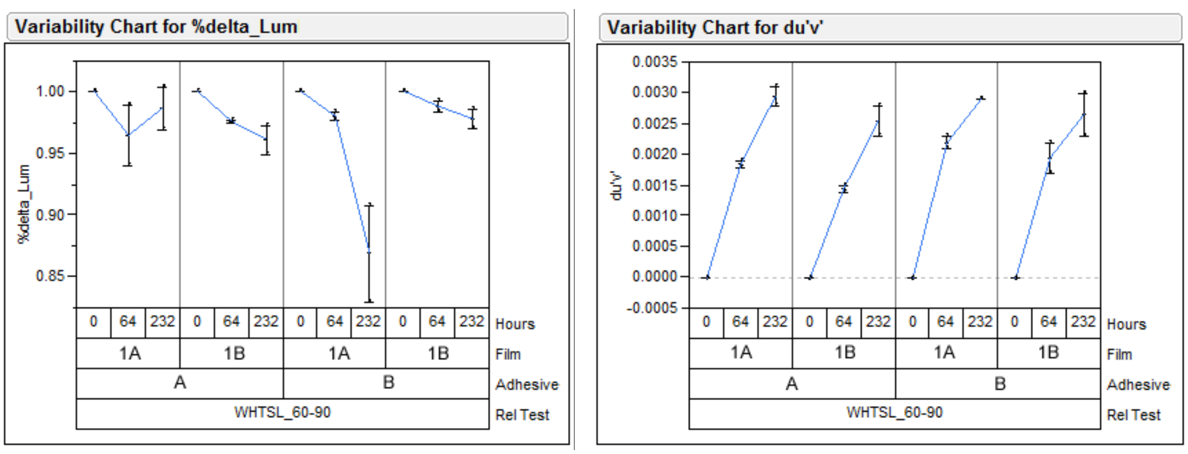

Fig. 30. Luminous flux (left) and color point (right) of adhesive-bonded lightguide-film samples subjected to WHTSL testing. By 274 hrs. both LF and color point of several samples had shifted by an unacceptable degree.

As we evolved the Light Module extraction scheme from features embedded in the lightguide surface to bonded extractors, we evaluated the luminance and color point uniformity (*i.e.* color mixing ability) of this newer approach. In general, it was observed that bonded extractors were superior in their ability to mix colors from LEDs with varying color point over angle. This was made possible due to the fact that each extractor acted as a “virtual source”: it collected light rays over a wide in-plane angular range, and effectively mixed these rays as they were re-directed via multiple lossless total internal reflections to the lit environment.

In Fig. 31 images recorded with a radiant imaging camera are shown, indicating the color uniformity achievable in an un-optimized LED-lightguide test setup, *i.e.* using “off-the-shelf” LEDs which were not tailored for lightguide coupling. Even for more widely spaced LEDs, the color point varied over the Light Module surface by < 0.002 in u’ and v’, *i.e.* less than two color point “steps”. This is promising for eventual Light Module manufacturing, since multiple LED color point bins could be utilized in the same module to achieve a desired net color point.

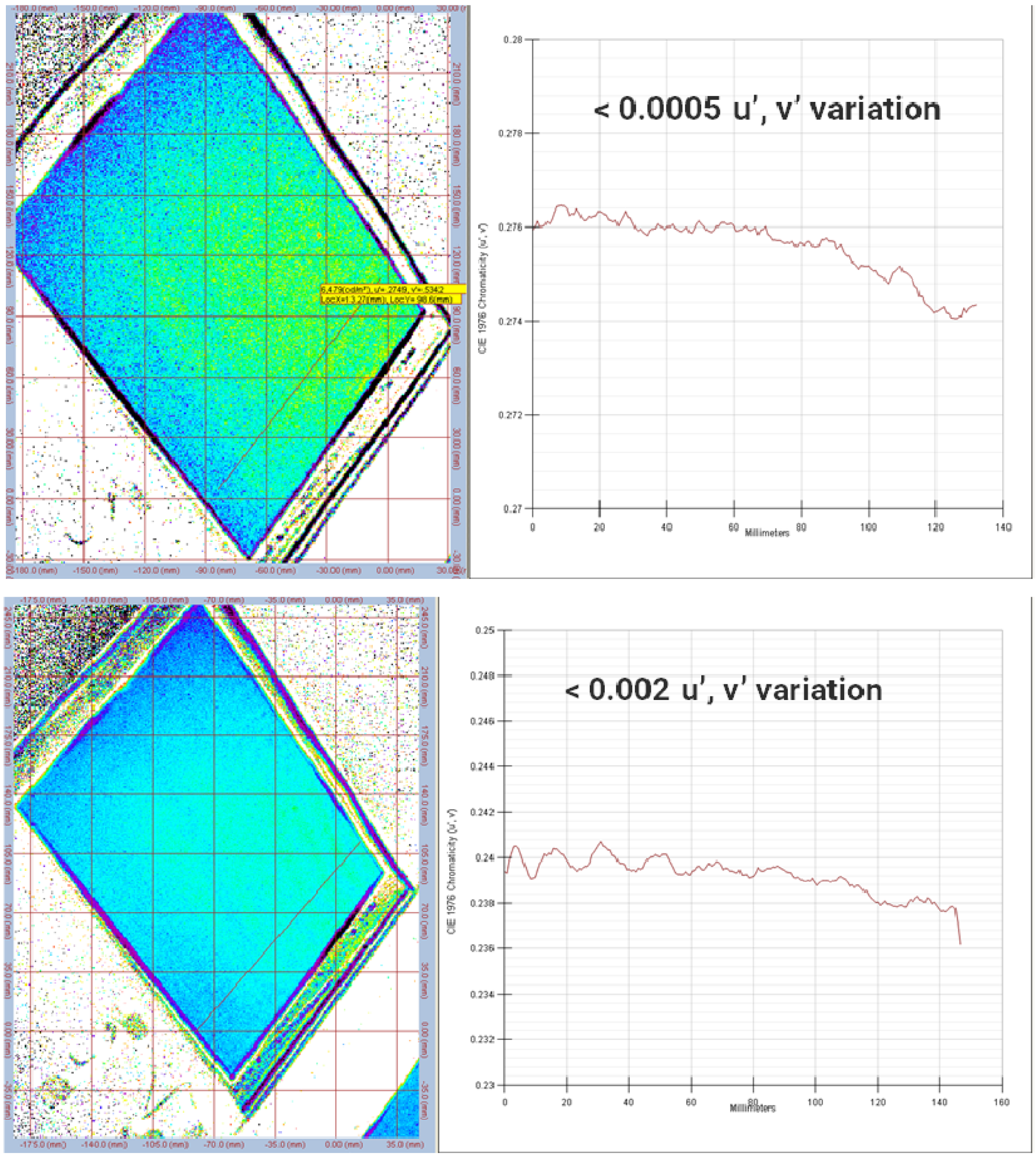

Fig. 31. Top: Radiometric image of a Light Module with XB-E LEDs spaced at a 4.5mm pitch, resulting in <0.0005 u’,v’ variation across the module surface. Bottom: the same module lit by XQ-B LEDs spaced at a wider 8mm pitch, resulting in <0.002 u’,v’ variation.

Task 4: Light Module Manufacturing Development

During Light Module fabrication process development we largely utilized commercially available liquid optically clear adhesives (OCAs), and had varying degrees of success in avoiding excessive wetting (meniscus formation) at extractor-lightguide junctions. As described above, we developed accelerated testing conditions relevant to the application stresses which luminaires composed of Light Modules would likely encounter. As an alternative to OCAs, which had mixed performance in our reliability test suite, we also investigated pressure-sensitive adhesives (PSAs) from three manufacturers, which are typically sold in the form of pre-formed thin sheets of uniform thickness. PSAs were appealing since they were expected to result in little to no meniscus formation. This was indeed the case, as indicated by the far-field intensity measurements in Fig. 32. The percent of light directed downward was higher by ~3% for PSAs relative to OCAs.

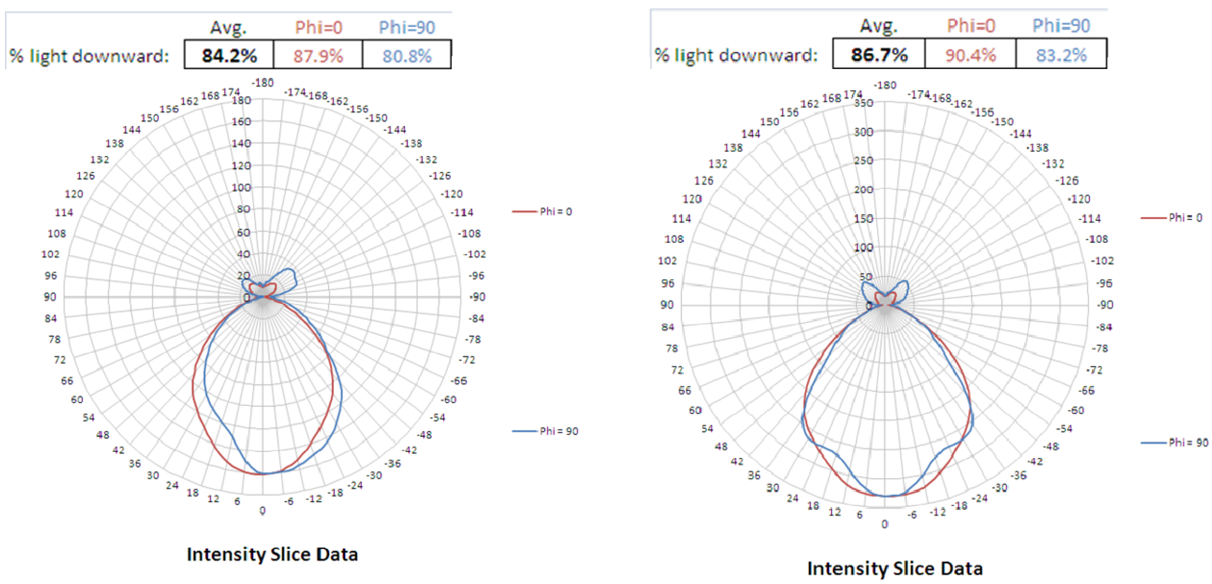

Fig. 32. Left: intensity over angle for apertured extractors bonded to a lightguide with optically clear adhesive, measured in two in-plane azimuths. Right: comparable measurement for pressure-sensitive adhesives.

However, it was found that on average, the bond strength of the PSAs was inadequate when compared to OCAs. This was demonstrated via peel testing, as shown in Fig. 33. Most PSA-bonded films delaminated from the lightguide at peak peel forces below 1 lbf, compared to >2 lbf for OCA-bonded films. This disparity increased when bonded films were stored at room temperature for several days, as the PSA-bonded films released more consistently at forces of < 1 lbf. Thus unless a PSA solution can be found which offers comparable strength to OCAs, the latter will be used for adhesive-based approaches.

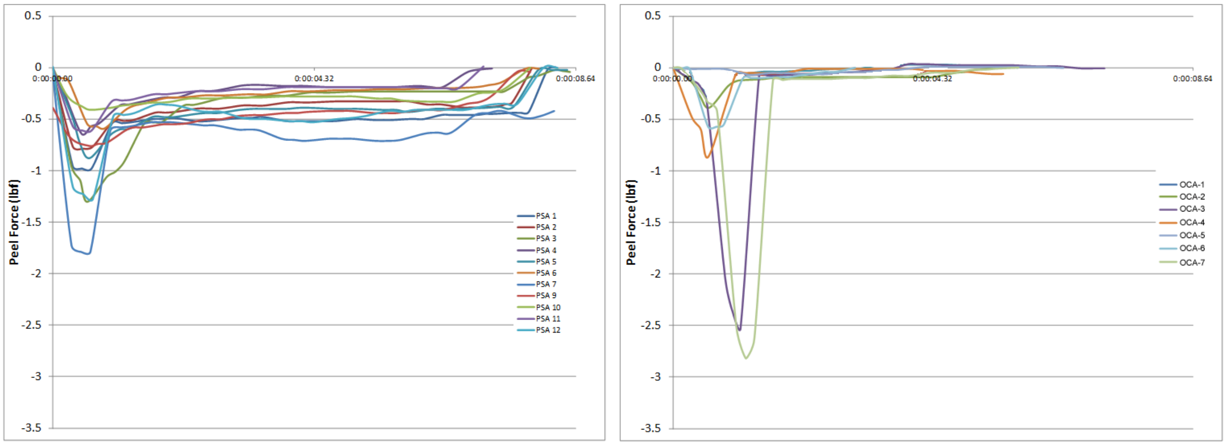

Fig. 33. Left: Mixed-mode peel strength of PSA-bonded extractor films; right: peel strength of corresponding OCA-bonded extractor films.

A key consideration throughout Light Module optical design as the feasibility and cost of fabrication as well as integration of light coupling and extraction features. As mentioned above, we transitioned to a bonded extraction scheme in which arrays of shaped extraction features were bonded to the lightguide. This approach presented advantages such as design flexibility and materials minimization, but only if the extraction features were of relatively small size (< 100µm), and their size and shape were uniform over large areas. These challenges were addressed via frequent input from Cree product development teams and interaction with several vendors.

Task 5: Luminaire Electrical and Mechanical Dev.

As part of luminaire electrical design, we developed a highly compact driver (AC to DC power converter) having a form factor compatible with low-profile luminaires incorporating the Light Module architecture. In addition to geometric design requirements, we also made high (> 90%) driver conversion efficiency a goal, since it directly affects overall system efficacy. To that end, we developed a high-frequency boost topology which can deliver 30-35W within a small volume. High frequency, enabled by a new microcontroller, made smaller inductor and capacitor sizes possible. As shown in Fig. 34, we built driver prototypes with dimensions of less than 9.0cm x 2.0cm x 1.5cm, which was of a size that makes integration into the luminaire frame feasible. Prototypes were tested over a wide frequency range, with 1-3 MHz (see Fig. 34) indicated as the optimal range at a 30-35W power level.

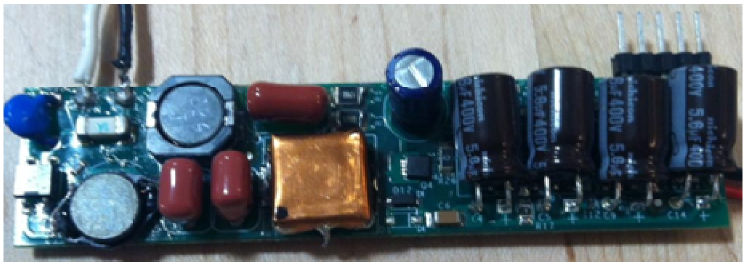

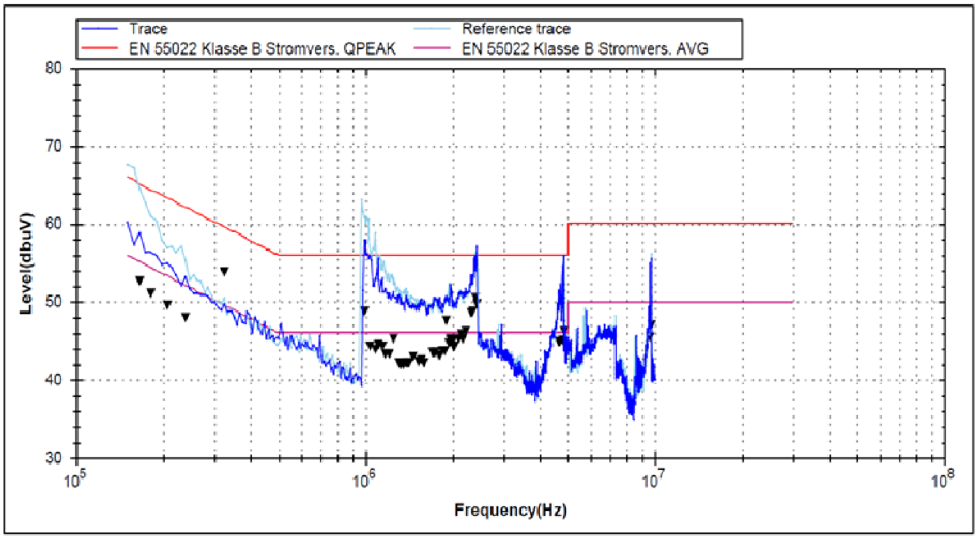

Fig. 34. Top: photograph of an assembled singled-side prototype driver circuit. Bottom: frequency scan indicating intended range of operation at 1-3 MHz.

The performance of the high-efficiency prototype driver is summarized in Table 1. These performance attributes met our design goals, and at a total estimated component cost of less than the $10 target set at the beginning of the program. Of particular note are the high peak efficiency (>94% at 30W), high power factor (> 0.98), and low electromagnetic noise which meets FCC requirements.

Table. 1. Summary of prototype driver performance attributes, which met all program design requirements.

Parameter	Spec
Input Voltage	120VAC
Output Voltage	240VDC
Output current regulation	<3%
Efficiency	**94% @ 30W**
PF	>0.98
THD	<20%
Power Density	1.3W/cm^3
EMI	Passes with C-L-C filter

As a key aspect of luminaire system-level design, we designed, built, and evaluated candidate mechanical structures enable by the Light Module concept. The design process was guided by the principles of: low profile; light weight; minimization of piece part number (and therefore bill of materials); and ease/speed of assembly. This resulted in design concepts which are compatible with the technical goals of the project, and which are also appealing and elegant from a design perspective. The concepts were of a 'boxless' design approach that represented a radical departure from typical pendants and troffers, which are typically composed of significant metal (enclosure and frame) content. In contrast, these new designs relied on lightguides as both optical and structural elements, with the result that they were much lighter than their metal-based counterparts. Although these concepts were not used for our end-of-project demonstration luminaire, they were evaluated for transition to Cree product development groups.

Task 6: Demo Luminaire with Light Module Integration

During Year 2 several different prototype luminaires utilizing Light Modules were designed and validated. Based on lessons learned from the design and fabrication processes for each, near the end of the program we began design work on the final demonstration luminaire. We originally proposed, and ultimately decided to fabricate, a 2' x 4' x 0.5" low-profile "panel" troffer design, as shown in Fig. 35. This luminaire consisted of 12 rectangular Light Modules in a "window pane" layout, with the remainder of the area made up of a lightweight aluminum frame. Compact LEDs were fabricated, tested, and incorporated into the Light Modules, after which all Modules were assembled into the frame. The luminaire was tested in a 2m integrating sphere to evaluate its performance relative to project targets.

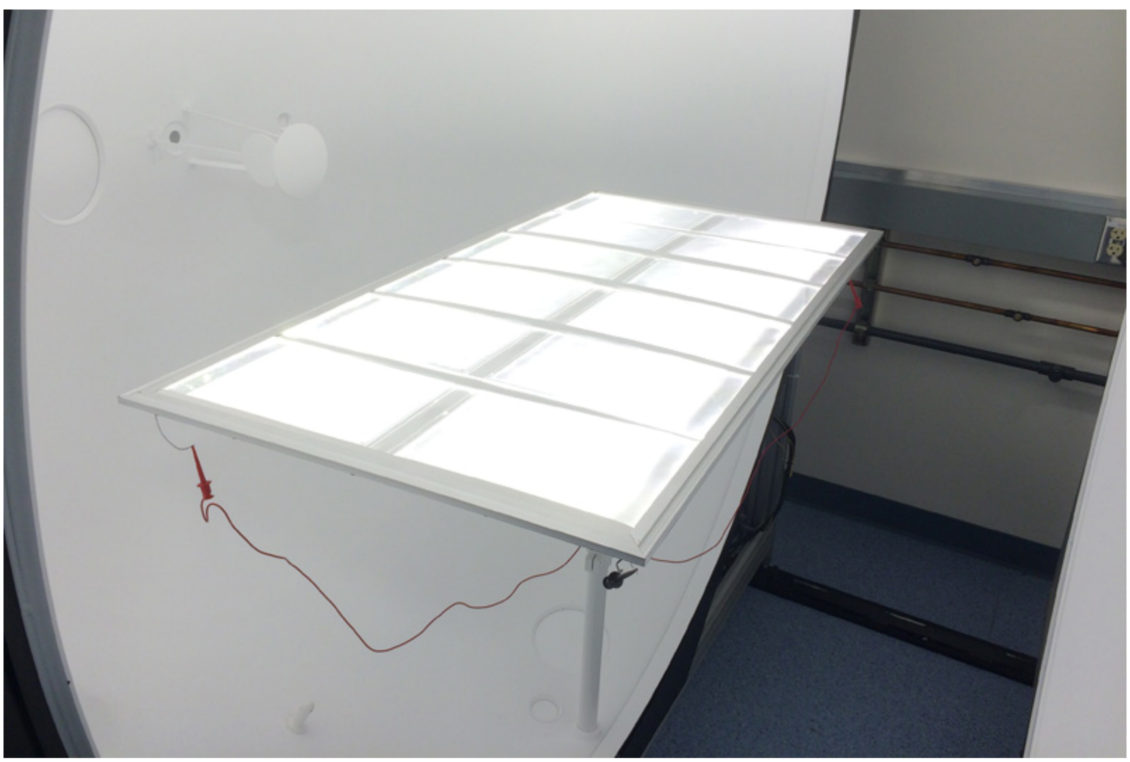

Fig. 35. Fully assembled demonstration luminaire in a 2m integrating sphere.

Before luminaire assembly, the LEDs were collectively evaluated in a smaller integrating sphere to measure their instant-on efficacy, total lumen output, color temperature, CRI, etc. The total LED luminous flux was used as the basis for determining the optical efficiency of the fully assembled luminaire. With the luminaire in the integrating sphere, its thermal efficiency (steady-state luminous flux over instant-on value) and electrical efficiency (efficacy with the driver installed, divided by the efficacy when powered directly by a DC power supply) were determined. The luminaire's characteristics are summarized in Table 2. All performance targets were met or exceeded, with the net stead-state efficacy of >135 lm/W significantly higher than our 116 lm/W goal. We believe that with further Light Module optimization (*e.g.* coupling efficiency of LEDs into the lightguide), the system optical efficiency could be raised by as much as 5%.

Table 2. Characteristics of Demonstration Luminaire

Characteristic	Value
Correlated Color Temperature (CCT)	3133
Distance from Blackbody Locus (Duv)	-0.003
Color Rendering Index (CRI)	91.8
Steady-State Luminous Flux (lm)	4190
Steady-State Luminous Efficacy (lm/W)	**135.4**
Optical Efficiency (target: >90%)	**90.2%**
Thermal Efficiency	98.8%
Driver Efficiency (target: >90%)	95.6%

A breakdown of estimated volume production cost contributions for the demonstration troffer was developed, and is provided in Table 3. The bill of materials (BOM) costs for the LED, optical, mechanical, and electrical subsystems of the demonstration troffer were estimated and adjusted for volume production discounts. Via input from Cree product development groups, the assembly and production overhead costs were also estimated. The cost breakdown indicates that no one subsystem appears to dominate the production cost. In addition, the modular optics design should result in total assembly costs which are lower than for conventional troffers. It was found that exclusive of shipping costs (variable based on location), the potential end-user average sales price (ASP) for this luminaire should be in the range of $100-115.

Table 3. Breakdown of estimated production cost contributions for the demonstration troffer.

Production Cost Category		Percent of Total
BOM	**LEDs**	22%
	Optical (Light Module)	16%
	Mechanical (frame, fasteners)	20%
	Electrical (PCBs, wires, driver)	15%
	Assembly	12%
	Overhead, Packaging, Freight	15%
	TOTAL	100%

Milestones / Deliverables

Technical milestones and deliverables are listed below, including anticipated start and completion dates vs. actual start and completion dates, as well as the status and percentage completion for each milestone/deliverable (where applicable).

Title: Demonstrate LED efficacy 140 lm/W at 25°C, 35 A/cm^2.
Success Criteria: Efficacy of 140 lm/W measured near a color temperature of 3000K on the black body locus, optionally at 90 CRI.
Planned Date: 2/1/14
Verification Method: Measure in a calibrated integrating sphere at SBTC.
Status: Completed on time, with an integrated TrueWhite (blue/yellow + red) package exhibiting a room-temperature "instant on" efficacy of ~145 lm/W at ~3000K and >90 CRI. A combined input power density of 1W/mm^2 was used in place of the typical DOE 35 A/cm^2 baseline current density, since the latter is difficult to define for both blue- and red-emitting chips in tandem.

Title: Model and verify intensity and color mixing capabilities of lightguide/extractor element.
Success Criteria: Achieve < 20% luminance variation over Light Module surface.
Planned Date: 2/1/14
Verification Method: Measure luminance using a calibrated imaging colorimeter.
Status: Completed early, with an estimated prototype lightguide showing an area-averaged luminance variation of 8-14% (depending on viewing angle), with no overlying diffuser.

Title: Reach LED efficacy of 150 lm/W at 25°C, 35 A/cm^2, 90 CRI.
Success Criteria: Efficacy of 150 lm/W measured near a color temperature of 3000K on the black body locus, at 90 CRI or higher.
Planned Date: 7/31/14
Verification Method: Measure in a calibrated integrating sphere at SBTC.
Status: Completed on time, using further optimization (*e.g.* chip size & arrangement) of the TrueWhite package described above.

Title: Develop high-throughput, high-yield selective LED phosphor application.
Success Criteria: LED color point variation < 0.007 in u',v' coordinates at 3000K CCT.
Planned Date: 7/31/14
Verification Method: Measure in a calibrated integrating sphere at SBTC.
Status: Completed on time, with a full-distribution variation in v' of <0.006 for selective downconverter application in a prototype integrated TrueWhite package.

Title: Down-select package substrate material based on cost, thermal properties.
Success Criteria: Compare two or more candidate substrate materials using quantitative metrics such as cost, yield, thermal conductivity, etc., and select the best candidate for future work.
Planned Date: 7/31/14
Verification Method: Quantified comparison of candidate material characteristics, using manufacturing-scale adjustments (*e.g.* lower cost at high volume) as appropriate.
Status: Completed on time. The per-component cost of a metal-coated silicon package substrate was estimated to be 10-15% higher than a corresponding ceramic substrate with composite reflective coating; the latter will be used for further development.

Title: Achieve substrate reflective coating with >90% reflectivity.
Success Criteria: Uniform substrate coating reflectivity of >90% in a wavelength range of 420-700nm.
Planned Date: 7/31/14
Verification Method: Calibrated reflectivity measurement in a spectrophotometer.
Status: Completed on time. A process for highly reflective metallic films on silicon substrates was developed, which includes a protective film to prevent reflectivity loss during high-T solder reflow.

Title: Verify reliability of prototype package.
Success Criteria: Achieve 90% LED lumen maintenance at 1,000 hrs. of standard Cree accelerated lifetime (reliability) testing.
Planned Date: 7/31/14
Verification Method: Expose prototype packages to high temperature / high humidity conditions and repeatedly measured luminous flux variation over time.
Status: Completed early. Multiple sets of integrated TrueWhite prototype LED packages passed this reliability criterion at 1,000 hrs.

Title: Design and build Light Module optics elements.
Success Criteria: Fabricate 6 x 6" Light Module with an optical efficiency of > 80% at >100 lm flux.
Planned Date: 7/31/14
Verification Method: In a calibrated integrating sphere, measure luminous flux of the fabricated Light Module relative to the corresponding flux from its centralized LED without any optics elements.
Status: Completed early. A 6x6" Light Module prototype was fabricated and tested, with a 94% optical efficiency (including diffuser) measured in an integrating sphere.

Title: Model and verify intensity and color mixing capabilities of lightguide/extractor element.
Success Criteria: Achieve < 0.005 u',v' color point variation over the Light Module surface.
Planned Date: 7/31/14
Verification Method: Measure spatial color point variation using a calibrated imaging colorimeter.
Status: Completed on time, based on several measurements using an imaging colorimeter.

Title: Achieve high Light Module optical efficiency with fully optimized compact high-efficacy/high-CRI LEDs.
Success Criteria: Achieve net Light Module optical efficiency of > 85%.
Planned Date: 7/31/14
Verification Method: In a calibrated integrating sphere, measure luminous flux of the fabricated Light Module relative to the corresponding flux from its centralized LED without any optics elements.
Status: Completed early, with a prototype light module exhibiting an optical efficiency of ~94% at ~100lm, including diffuser loss.

Title: Develop manufacturing processes for optimized Light Module subsystems.
Success Criteria: Identify two or more viable candidate manufacturing processes.
Planned Date: 7/31/14
Verification Method: Identify and compare at least two candidate manufacturing processes for the Light Module optics elements.
Status: Completed on time. Two candidate manufacturing processes have been identified for the lightguide extraction features, with a third under consideration as well. Candidate manufacturing processes for the coupling cavity are still undecided, since the geometry of the cavity will influence which process(es) would be best suited to mass manufacture.

Title: Define critical feature dimensions and tolerances.
Success Criteria: Identify key feature dimension and tolerances for optimized Light Module.
Planned Date: 11/1/14
Verification Method: Via fabrication test runs and dimensional characterization, determine tolerance (and smallest feature) limitations of candidate manufacturing processes.
Status: Completed on time. For the apertured extraction scheme we have determined not only key feature dimensional tolerances, but also adhesive shape tolerances.

Title: Develop low-cost electrical interconnection scheme for low-profile luminaires.
Success Criteria: Identify two or more candidate electrical interconnect schemes.
Planned Date: 11/1/14
Verification Method: Based on a survey of commercially available solutions as well as approaches developed in house, identify at least two candidate low-profile electrical interconnect schemes. Develop relevant selection criteria such as cost per unit area, thermal resistance, etc.
Status: Completed on time. It was found that for likely luminaire form factors, conventional low-cost printed circuit boards will be adequate for thermal management of LED arrays.

Title: Complete LED substrate die attach and thermal shock reliability testing.
Success Criteria: Chip solder attach yield should meet or exceed that of standard Cree packages.
Planned Date: 2/1/15
Verification Method: Measure shear strength of soldered chips to substrate, and repeatedly measure forward voltage variation during numerous cycles of thermal shock testing.
Status: Completed ahead of schedule.

Title: Develop manufacturing processes for optimized Light Module subsystems.
Success Criteria: Identify key limitations of each candidate Light Module manufacturing process.
Planned Date: 2/1/15
Verification Method: Consult with Cree manufacturing colleagues and vendors to identify key limitations of candidate Light Module optics element manufacturing techniques, such as cost, yield, tolerances, and reproducibility.
Status: Completed on time, with adhesive and thermally bonded approaches compared in various respects.

Title: Design and build compact and efficient electrical driver.
Success Criteria: Identify driver topology and drive frequency range to be employed.
Planned Date: 2/1/15

Verification Method: Using anticipated prototype LED voltage/current characteristics as well as the total number of LEDs, determine a driver topology (architecture), including frequency range, which will enable reaching final 90% driver efficiency target.
Status: Completed ahead of schedule. A high-frequency driver topology enabling compact driver size at high (94%) AC-DC conversion efficiency was developed.

Title: Design and build lightweight mechanical structure for low-profile, broad-area luminaires.
Success Criteria: Develop two or more candidate mechanical housing designs.
Planned Date: 2/1/15
Verification Method: Based on anticipated low-profile luminaire geometry and structural requirements, develop at least two candidate mechanical housing designs which contribute to light weight and low cost of the final demonstration luminaire.
Status: Completed on time via design and prototyping of three Light Module-based luminaires.

Title: Design and fabricate 6 x 6" or larger Light Module.
Success Criteria: Fabricate 6 x 6" Light Module with an optical efficiency of > 90% at >150 lm flux.
Planned Date: 5/1/15
Verification Method: In a calibrated integrating sphere, measure luminous flux of the fabricated Light Module relative to the corresponding flux from its centralized LED without any optics elements.
Status: Completed early. A 6x6" Light Module prototype was fabricated and tested, with a 94% optical efficiency (including diffuser) measured in an integrating sphere.

Title: Model and verify intensity and color mixing capabilities of lightguide/extractor element.
Success Criteria: Achieve < 10% luminance variation over Light Module surface.
Planned Date: 5/1/15
Verification Method: Measure luminance using a calibrated imaging colorimeter.
Status: Completed on time, confirmed with radiant imaging camera.

Title: Achieve high optical efficiency with fully optimized compact high-efficacy/high-CRI LEDs.
Success Criteria: Achieve net Light Module optical efficiency of > 90%.
Planned Date: 5/1/15
Verification Method: In a calibrated integrating sphere, measure luminous flux of the fabricated Light Module relative to the corresponding flux from its centralized LED without any optics elements.
Status: Completed early. A 6x6" Light Module prototype was fabricated and tested, with a 94% optical efficiency (including diffuser) measured in an integrating sphere.

Title: Define critical feature dimensions and tolerances.
Success Criteria: Based on testing, modify critical dimensions/tolerances and verify > 90% optical efficiency is maintained.
Planned Date: 5/1/15
Verification Method: If necessary and based on input from dimensional tolerance analysis, modify optical elements design(s) to verify that 90% or greater optical efficiency (as measured in

an integrating sphere) is maintained.
Status: Completed on time, via a combination of modeling and discussions with extractor sheet manufacturers.

Title: Develop low-cost electrical interconnection scheme for low-profile luminaires.
Success Criteria: Down-select to one electrical interconnect scheme based on reliability testing and cost factors.
Planned Date: 5/1/15
Verification Method: Based on empirical and theoretical comparison, choose an electrical interconnect scheme for the demonstration luminaire which contributes to end-of-program goals such as low cost.
Status: Completed ahead of schedule. It was found that for likely luminaire form factors, conventional low-cost printed circuit boards will be adequate for thermal management of LED arrays.

Title: Design and build compact and efficient electrical driver.
Success Criteria: Achieve 90% driver electrical efficiency at estimated cost of < $10.
Planned Date: 5/1/15
Verification Method: Fabricate a compact electrical driver with > 90% efficiency at an estimated cost (adjusted for production volumes) of $10 or less.
Status: Completed ahead of schedule, with 94% conversion efficiency demonstrated.

Title: Design and build lightweight mechanical structure for low-profile, broad-area luminaires.
Success Criteria: Down-select to one mechanical design based on rigidity, cost, and weight.
Planned Date: 5/1/15
Verification Method: Develop quantitative metrics for comparison of luminaire mechanical designs, and select one that best contributes to program goals of low cost and high production throughput.
Status: Completed on time.

Title: LED efficacy of 162 lm/W at 25°C, 35 A/cm^2, 90 CRI, 3000K CCT.
Success Criteria: Efficacy of 162 lm/W at a color temperature of 3000K on the black body locus, at 90 CRI or higher.
Planned Date: 7/31/15
Verification Method: Measure in a calibrated integrating sphere at SBTC.
Status: Not reached. An LED efficacy of ~151 lm/W was achieved for these conditions.

Title: Develop high-throughput, high-yield selective LED phosphor application.
Success Criteria: LED color point variation < 0.005 in u',v' coordinates at 3000K CCT.
Planned Date: 7/31/15
Verification Method: Measure in a calibrated integrating sphere at SBTC.
Status: Not started. De-prioritized due to change in package configuration.

Title: Achieve substrate reflective coating with >95% reflectivity.
Success Criteria: Uniform substrate coating reflectivity of >95% in a wavelength range of 420-700nm.

Planned Date: 7/31/15
Verification Method: Calibrated reflectivity measurement in a spectrophotometer.
Status: Completed early. A process for highly reflective metallic films on silicon substrates was developed, which includes a protective film to prevent reflectivity loss during high-T solder reflow.

Title: Verify reliability of prototype package.
Success Criteria: Achieve 95% LED lumen maintenance at 1,000 hrs. of standard Cree accelerated lifetime (reliability) testing.
Planned Date: 7/31/15
Verification Method: Expose prototype packages to high temperature / high humidity conditions and repeatedly measured luminous flux variation over time.
Status: Completed ahead of time. Prototype LEDs with an HRI formulation subjected to HTOL testing passed 1,000 hrs. with <5% LF drop.

Title: Model and verify intensity and color mixing capabilities of lightguide/extractor element.
Success Criteria: Achieve < 0.002 u',v' color point variation over the Light Module surface.
Planned Date: 7/31/15
Verification Method: Measure spatial color point variation using a calibrated imaging colorimeter.
Status: Completed on time; confirmed with radiant imaging camera.

Title: Develop manufacturing processes for optimized Light Module subsystems.
Success Criteria: Down-selection to one Light Module manufacturing process based on estimated cost and yield.
Planned Date: 7/31/15
Verification Method: Based on quantitative comparison of metrics for candidate manufacturing techniques (*e.g.* cost per unit area, anticipate yield), select one which presents the best prospects for large-scale manufacture of Light Module optics elements.
Status: Completed on time; the cost and yield of likely fabrication techniques was evaluated.

Title: Assemble and test 2' x 4'demonstration luminaire based on Light Modules.
Success Criteria: Build 2' x 4' panel luminaire of < 0.5" thickness, with 4000 lm output at 116 lm/W, a CRI of > 90, and a 3000K CCT.
Planned Date: 7/31/15
Verification Method: Quantify luminaire performance in an integrating sphere at SBTC, and optionally verify at a large integrating sphere at Cree Durham.
Status: Completed one month late. Luminaire performance targets were met or exceeded.

Title: Final estimation of assembled luminaire costs and end-user price.
Success Criteria: Demonstrate cost breakdown structure that leads to a $120 end-user price for the demonstration luminaire.
Planned Date: 7/31/15
Verification Method: Calculate the cost contributions of the various luminaire subsystems (adjusted for volume production and taking production overhead into account), and demonstrate the feasibility an end-user price of $120 or less, given a representative profit margin.

Status: Completed one month late. It was found that estimated demonstration troffer costs should lead to an ASP of <$120.

IMPACT, PRODUCTS

A chief project accomplishment was the development of a scalable, versatile Light Module concept based on the use of thin light guides with dense arrays of smart light extractors. Cree foresees this as being the basis for future solid-state luminaire designs which offer high efficacy and color quality at low comparative cost to existing products. It is likely that by further building on the Light Module approach, Cree will develop LED-based luminaires which offer superior normalized cost ($/klm) to fluorescent fixtures.

During the program a U.S. patent application was filed on 8/28/14, entitled "Extraction Film for Optical Lightguide and Method of Producing Same", with U.S. patent application number 14/471,991 and U.S. patent publication number US 2015/0192742 A1.